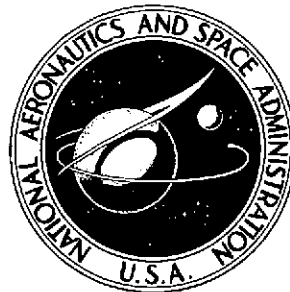


P.M.W.

NASA TECHNICAL NOTE



NASA TN D-7594

NASA TN D-7594

(NASA-TN-D-7594) AN INTEGRAL EQUATION
FORMULATION FOR PREDICTING RADIATION
PATTERNS OF A SPACE SHUTTLE ANNULAR SLOT
ANTENNA (NASA) 81 p HC \$4.00 CSCL 17B

N74-29498

Unclassified
45606



AN INTEGRAL EQUATION FORMULATION FOR PREDICTING RADIATION PATTERNS OF A SPACE SHUTTLE ANNULAR SLOT ANTENNA

by J. Earl Jones and J. H. Richmond

Langley Research Center
Hampton, Va. 23665



NATIONAL AERONAUTICS AND SPACE ADMINISTRATION • WASHINGTON, D. C. • AUGUST 1974

1. Report No. NASA TN D-7594	2. Government Accession No.	3. Recipient's Catalog No.	
4. Title and Subtitle AN INTEGRAL EQUATION FORMULATION FOR PREDICTING RADIATION PATTERNS OF A SPACE SHUTTLE ANNULAR SLOT ANTENNA		5. Report Date August 1974	
7. Author(s) J. Earl Jones and J. H. Richmond		6. Performing Organization Code	
9. Performing Organization Name and Address NASA Langley Research Center Hampton, Va. 23665		8. Performing Organization Report No. L-9279	
12. Sponsoring Agency Name and Address National Aeronautics and Space Administration Washington D.C. 20546		10. Work Unit No. 502-33-13-01	
		11. Contract or Grant No.	
		13. Type of Report and Period Covered Technical Note	
		14. Sponsoring Agency Code	
15. Supplementary Notes <p>This work was partially supported under NASA Grant NGL-36-008-138 to the ElectroScience Laboratory, The Ohio State University. Part of this work was presented at the 1972 International Antenna and Propagation Symposium, Williamsburg, Virginia, December 11-15, 1972.</p> <p>J. H. Richmond is a professor of Electrical Engineering, The Ohio State University, Columbus, Ohio.</p>			
16. Abstract <p>An integral equation formulation is applied to predict pitch- and roll-plane radiation patterns of a thin VHF/UHF (very high frequency/ultra high frequency) annular slot communications antenna operating at several locations in the nose region of the Space Shuttle orbiter. Digital computer programs used to compute radiation patterns are given and the use of the programs is illustrated. Experimental verification of computed patterns is given from measurements made on 1/35-scale models of the orbiter.</p>			
17. Key Words (Suggested by Author(s)) Prediction of radiation patterns Spacecraft antennas Annular slot antennas		18. Distribution Statement Unclassified - Unlimited	
		STAR Category 07	
19. Security Classif. (of this report) Unclassified	20. Security Classif. (of this page) Unclassified	21. No. of Pages 81	22. Price* \$4.00

* For sale by the National Technical Information Service, Springfield, Virginia 22151

AN INTEGRAL EQUATION FORMULATION FOR PREDICTING
RADIATION PATTERNS OF A SPACE SHUTTLE
ANNULAR SLOT ANTENNA¹

By J. Earl Jones and J. H. Richmond²
Langley Research Center

SUMMARY

A synopsis is presented of a recently developed, integral equation formulation for predicting radiation patterns of thin axial slot antennas mounted on an infinitely long, perfectly conducting cylinder of arbitrary cross section. The method is applied to compute radiation patterns in both the pitch and roll planes of a thin VHF/UHF (very high frequency/ultra high frequency) annular slot communications antenna operating at several locations in the nose region of the Space Shuttle orbiter. Digital computer programs used to compute radiation patterns are also given and the use of the programs is illustrated. Experimental verification of computed patterns is given from measurements made on 1/35-scale models of the orbiter.

The results indicate that even when formulated for two-dimensional bodies, the integral equation formulation is useful for predicting principal plane radiation patterns of antennas mounted on moderate to large electrical size bodies such as the Space Shuttle orbiter. The upper limit of the perimeter of the body is dependent on the size of the digital computer used to make the computations. For the computer employed, the maximum perimeter was found to be from 30 to 36 wavelengths.

INTRODUCTION

The Space Shuttle is a reusable NASA vehicle that is expected to receive considerable attention in the forthcoming decade. The motivation for the development of the Space

¹This work was supported in part by the National Aeronautics and Space Administration, Langley Research Center, Hampton, Virginia 23665, under Grant NGL-36-008-138 to the ElectroScience Laboratory, The Ohio State University, Columbus, Ohio 43212. Part of this work was also presented at the 1972 International Antenna and Propagation Symposium in Williamsburg, Virginia, December 11-15, 1972.

²Professor of Electrical Engineering, The Ohio State University, Columbus, Ohio.

Shuttle is the reduction in cost of launching spacecraft into earth orbit and the transportation of men and supplies to and from orbiting space stations. Reusability is achieved by allowing the vehicle to take off like a rocket and to land like an airplane. Thus, the Space Shuttle will require a large number of antennas, since aircraft-type landing and navigation antennas will be needed in addition to the usual spacecraft antennas. Moreover, since the vehicle surface will be at extreme temperatures during atmospheric reentry, antenna locations must be selected in regions where minimum temperatures are anticipated, as well as in regions where structural impact is minimal.

Space Shuttle antennas must possess specific performance characteristics, that is, radiation patterns, impedance, and so forth, in order for desired mission objectives to be achieved. A purely experimental design approach for one antenna would be to (a) construct many scale models of the orbiter, each model containing a proposed antenna geometry at a proposed location, (b) conduct performance measurements, and (c) conclude by selecting the geometry and location giving the most desirable data. However, for Space Shuttle antenna design, this approach has two disadvantages: (a) excessive time and cost are required to construct many models and to conduct many measurements, and (b) changes in the geometry of the vehicle, which is currently only in early design stages, would necessitate the construction and testing of new models to determine whether the antenna performance remains adequate.

A more desirable approach to Space Shuttle antenna design would be to apply theoretical methods which would provide some indication of antenna performance. Easily adaptable to a digital computer, such methods could then be used to compute antenna performance for a wide variety of conditions of antenna geometry and location on the vehicle surface. The design parameters yielding desirable theoretical performance data could then be used to construct a scale model for final checkout. Not only are excessive model construction and testing avoided in this approach, but also the time required to ascertain the influence of a vehicle geometry design change is significantly reduced.

The two basic theoretical methods believed to provide the most useful insight into Space Shuttle antenna design are (a) the integral equation formulation (IEF) (refs. 1 to 5) and (b) the geometrical theory of diffraction (GTD) (refs. 6 to 9). Both IEF (refs. 10 to 12) and GTD (refs. 13 to 16) have recently been used with success in the design of spacecraft and aircraft antennas, and the advantages and limitations of each method are well-documented (ref. 17). Even though GTD and IEF are inherently useful for analyzing antennas mounted on electrically large and electrically small bodies, respectively, the nature of the Space Shuttle antenna design will require the application of both methods. Furthermore, since there is usually a range of body electrical size for which both GTD and IEF are applicable (ref. 17), the use of both methods serves as a check case.

In this paper, an IEF recently developed by Richmond (ref. 5) hereafter designated as the "Richmond Integral Equation Formulation" (RIEF), is briefly described and applied to predict radiation patterns in both the pitch and roll planes of a thin VHF/UHF annular slot communications antenna operating at several locations in the nose region of the Space Shuttle orbiter. Radiation patterns computed by RIEF are given for selected cases. Experimental verification for RIEF is given from radiation pattern measurements made with 1/35-scale models of the Space Shuttle orbiter, and the merits and limitations of RIEF for Space Shuttle antenna design are discussed.

The digital computer programs used for computing radiation patterns are given in appendix A. Finally, an example illustrating the use of the programs is given in appendix B.

SYMBOLS

a	mean radius of annular slot
d_I	inner diameter of annular slot
d_M	mean diameter of annular slot
d_n	length of segment n
d_O	outer diameter of annular slot
\bar{E}	electric field vector in annular slot aperture
\bar{E}_i	electric field radiated by strip vee dipole i
E_ϕ	radiation field
[I]	$N \times 1$ (column) matrix of unknown dipole mode currents
I_n	current per unit length at point P_n
i	index of point, segment, strip vee dipole
\bar{J}_{Dn}	surface current density along strip vee dipole n

\bar{J}_n	surface current density along segment n
j	index of point, segment, strip vee dipole
k	free-space propagation constant
N	number of points, number of segments, number of strip vee dipoles, number of simultaneous equations
N'	number of coarse points
n	index of point, segment, strip vee dipole
n_1, n_2, n_3, n_4, n_5	dimensioning integers
P_n	point of intersection between segments $n - 1$ (segment N for $n = 1$) and n
\hat{s}_n	orientation unit vector of segment n
t_j	distance from point P_{j-1} along strip vee dipole j
t_n	distance along segment n from point P_n
t_{n-1}	distance along segment $n-1$ from point P_{n-1}
[V]	$N \times 1$ (column) excitation matrix
V_n	voltage of point P_n
x,y	distances along X- and Y-axes
\hat{x}, \hat{y}	vector notation for X- and Y-axes
x_n, y_n	distances of point P_n along X- and Y-axes
[Z]	$N \times N$ matrix of impedance coefficients

Z_{ij}	free-space mutual impedance between strip vee dipole i and strip vee dipole j
α_n, β_n	direction angles of segment n
λ	free-space wavelength
ϕ	reference angle
ϕ_p	pitch-plane reference angle
ϕ_r	roll-plane reference angle

CONFIGURATION

An annular slot antenna having an inner diameter of 48.37 cm and an outer diameter of 58.31 cm and radiating over the frequency range of 150 to 400 MHz is to be considered for operation at the points A, B_1 , and B_2 , as indicated in figure 1 on a diagram of the Space Shuttle orbiter. The roll and pitch planes in which radiation patterns are to be determined, as well as the roll-plane reference angle ϕ_r and the pitch-plane reference angle ϕ_p , are also defined in figure 1. Roll-plane patterns are to be obtained for the annular slot excited at A (designated as case 1 throughout this paper) and at B_1 (case 2), and simultaneously excited at B_1 and B_2 (case 3). Pitch-plane patterns are also to be obtained for the annular slot excited at A (case 4).

Since the orbiter is electrically large over the required operating frequency range, a reasonable approximation is to assume the roll-plane pattern to be the pattern produced by an annular slot located on an infinitely long, perfectly conducting cylinder of the same cross section as the cross section of the orbiter in the plane containing the points A, B_1 , and B_2 and perpendicular to the longitudinal axis of the orbiter. Similarly, it is reasonable to assume the pitch-plane pattern to be the pattern produced by an annular slot located on an infinitely long, perfectly conducting cylinder having the same cross section as the cross section of the orbiter in the plane containing point A and the longitudinal axis of the orbiter. However, since the size of the orbiter in the pitch plane exceeds the limitations of RIEF, a foreshortened approximation (to be explained later) is used for the pitch-plane cross section in order to make pattern computations.

INTEGRAL EQUATION FORMULATION

Richmond (ref. 5) has recently developed a Galerkin's method IEF solution (RIEF) and a user-oriented digital computer program for computing the radiation pattern of one or more axial slot antennas mounted on a conducting cylinder of infinite length and arbitrary cross section. The slot antennas may be either narrow (with infinitesimal width) or wide (with finite width). For simplicity, application of RIEF in this paper is for several narrow axial slots mounted on a perfectly conducting cylinder, the geometry of which is shown in figure 2. The electromagnetic field is assumed to be transverse electric (TE) to the cylinder axis; thus, the radiation field consists of only the E_ϕ component. A synopsis of RIEF is given in this paper; further details are given in reference 5.

In RIEF, the cylinder cross-section profile is initially subdivided into a specified number N of straight segments, as shown in figure 2. The point of intersection P_n ($n = 1, 2, \dots, N$) of any two adjacent segments³ n and $n + 1$ is regarded as a "delta gap" across which a known voltage V_n may exist for excitation of the structure. Points for which $V_n \neq 0$ are interpreted as narrow axial slots so that in the subdivision process any narrow axial slot on the cylinder is required to be located at a point of intersection.

Segment n ($n = 1, 2, \dots, N$) is characterized by the end points $P_n = (x_n, y_n)$ and $P_{n+1} = (x_{n+1}, y_{n+1})$, segment length $d_n = [(x_{n+1} - x_n)^2 + (y_{n+1} - y_n)^2]^{1/2}$, and orientation unit vector $\hat{s}_n = \cos \alpha_n \hat{x} + \cos \beta_n \hat{y}$ directed from P_n to P_{n+1} , where $\cos \alpha_n = (x_{n+1} - x_n)/d_n$ and $\cos \beta_n = (y_{n+1} - y_n)/d_n$. For accurate radiation pattern computations, all segments should be no greater than $\lambda/4$ in length where λ is the free-space wavelength. Accuracy is enhanced, however, if the length is moderately shorter than $\lambda/4$, especially for segments close to a narrow axial slot.

Any two adjacent segments represent the arms of a strip vee dipole; in particular, segments $n - 1$ and n constitute strip vee dipole n , as indicated in figure 2. In all, there are N overlapping strip vee dipoles. A useful representation for the surface current distribution on dipole n is the piecewise sinusoidal representation

$$\bar{J}_{Dn}(t) = I_n \frac{\sin kt_{n-1}}{\sin kd_{n-1}} \hat{s}_{n-1} \quad (0 \leq t_{n-1} \leq d_{n-1}) \quad (1a)$$

$$\bar{J}_{Dn}(t) = I_n \frac{\sin k(d_n - t_n)}{\sin kd_n} \hat{s}_n \quad (0 \leq t_n \leq d_n) \quad (1b)$$

³Since the array of segments in figure 2 is a closed array of segments, the index $n + 1$ must be replaced by 1 for $n = N$, and the index $n - 1$ must be replaced by N for $n = 1$.

where t_{n-1} is the distance from P_{n-1} along segment $n - 1$ and t_n is the distance from P_n along segment n , and where $k = 2\pi/\lambda$. From equations (1), the resultant surface current distribution on segment n is given by

$$\bar{J}_n(t) = \frac{[I_{n+1} \sin kt_n + I_n \sin k(d_n - t_n)]}{\sin kd_n} \hat{s}_n \quad (0 \leq t_n \leq d_n) \quad (2)$$

where t_n is the distance from P_n along segment n .

The end point surface current densities I_n ($n = 1, 2, \dots, N$) which are unknown quantities are determined by solving the system of N simultaneous equations

$$[Z][I] = [V] \quad (3)$$

where $[Z]$ is a $N \times N$ impedance coefficient matrix which can be determined (ref. 5), $[I]$ is the $N \times 1$ (column) matrix of unknown dipole mode currents, and $[V]$ is the $N \times 1$ (column) excitation matrix, the elements of which are nonzero only for actual slots. The Z_{ij} ($i, j = 1, 2, \dots, N$) in $[Z]$ physically represent the free-space mutual impedance between strip vee dipole i and strip vee dipole j under the condition for which the current distribution on each dipole is piecewise sinusoidal. Thus,

$$Z_{ij} = -\frac{1}{I_i I_j} \left[\int_0^{d_{j-1}} \bar{E}_i(t_{j-1}) \cdot \bar{J}_{Dj}(t_{j-1}) dt_{j-1} + \int_0^{d_j} \bar{E}_i(t_j) \cdot \bar{J}_{Dj}(t_j) dt_j \right] \quad (4)$$

where \bar{E}_i is the electric field radiated by dipole i due to the current distribution \bar{J}_{Di} given by equations (1) and evaluated on the surface of dipole j (the surface of and points interior to dipole j are assumed to be replaced by free space), \bar{J}_{Dj} is also given by equations (1), and t_j is the distance from P_{j-1} along segment j . Details for computing Z_{ij} are given in reference 5.

The solution for $[I]$ yields the coefficients I_n needed in equation (2) for the computation of the current distribution on the cylinder. Standard techniques are then employed to compute the radiation field E_ϕ . Patterns are computed with the coordinate origin 0 as the phase center.

REPRESENTATION OF AN ANNULAR SLOT

In order for the roll- and pitch-plane patterns of the annular slot in figure 1 to be computed, subject to the approximations given, the radiation pattern of a thin annular slot located on an infinitely long, perfectly conducting, noncircular cylinder must be computed in a plane perpendicular to the axis of the cylinder and containing the center of the

annular slot, as shown in figure 3. Under the assumption that the field in the annular slot aperture is transverse electric and magnetic (TEM) to the aperture, \bar{E} on any radial line of the slot aperture is equal in amplitude and opposite in phase to \bar{E} on the diametrically opposite radial line. Consequently, application of RIEF for narrow axial slots requires that the annular slot be simulated, as shown in figure 3, by an equivalent array of two infinitely long, antiphase narrow axial slots of equal amplitude, and spaced by the distance $d_M = (d_I + d_O)/2$, where d_I and d_O are the inner and outer diameters, respectively, of the annular slot.

EXPERIMENTAL MODELS

Two 1/35-scale models were constructed for obtaining radiation patterns experimentally. The first model, shown in figure 4, is a cylindrical model having a cross section similar to the cross section of the orbiter in the roll plane. The second model, shown in figure 5, is a three-dimensional model with the side and front views clearly showing the pitch- and roll-plane cross-section profiles, respectively. For the scale models, the annular slot inner diameter scales to 1.382 cm and the outer diameter scales to 1.666 cm, and the frequency range⁴ of 150 to 400 MHz scales to 5.250 to 14.000 GHz. For each model, the location of the annular slot antenna corresponds to point A of figure 1; consequently, the cylindrical model may be used to obtain radiation patterns only for case 1 and the three-dimensional model may be used to obtain radiation patterns only for cases 1 and 4.

Since RIEF is directly applicable only for two-dimensional models, the purpose of the cylindrical model is to verify RIEF experimentally. The infinitely long cylinder assumed in RIEF is simulated experimentally by a cylinder of length 39.04 cm, as shown in figure 4. This length is 6.83 wavelengths at the lowest desired scaled frequency of 5.250 GHz.

NUMERICAL COMPUTATIONS AND EXPERIMENT

RIEF was applied to obtain computations of the radiation patterns for cases 1 to 4. Computations were made over the scaled frequency range for the 1/35-scale model. For each pattern computation, only a coarse number N' ($N' \leq N + 1$) of points were initially specified. The remaining points P_n , particularly those in the shadow region of the slot(s), were automatically selected with the aid of a spline curve fit procedure. This procedure not only reduces the number of input data points but also is desirable in order

⁴In this paper, frequencies given in GHz refer to the 1/35-scale models; and those given in MHz refer to the full-scale structure.

that a smooth profile be obtained, since in most cases the points must be read graphically from drawings and inaccuracies in profile smoothness often result.

The digital computer programs which were used to obtain radiation pattern computations are given in appendix A. An example illustrating the use of the programs is given in appendix B.

The upper limit of the perimeter of a cylinder which can be analyzed with RIEF is dependent on the storage capacity of the computer used to obtain computations, which, in this paper, were made on a Control Data Corporation 6600 computer at NASA Langley Research Center. It was found that for this computer and for the auxiliary plotting programs employed, the maximum number of simultaneous equations which could be solved without exceeding storage capacity was 180. Under this condition, the upper limit of the perimeter is from 30 to 35 wavelengths, and the running time for a typical pattern (1° increments) is about 100 seconds.

Roll-Plane Radiation Patterns

The roll-plane cross section in the plane containing the points A , B_1 , and B_2 is described for case 1 by 154 points shown in figure 6. When these points are connected, a polygon of perimeter 70.58 cm is formed, and 154 simultaneous equations are solved to compute the radiation pattern.

The geometry for cases 2 and 3 is shown in figures 7 and 8, respectively. The point locations in figures 7 and 8 are similar to the point locations in figure 6, except that in figures 7 and 8 additional points were added in the vicinity of the sources. This procedure is necessary to obtain more reliable data for cases 2 and 3. The perimeter, number of points and simultaneous equations, the scaled coordinates of the center of the annular slots, and the scaled coordinates and voltage strengths of the equivalent axial slots are conveniently presented for each case in table I.

Experimental verification for the roll-plane patterns was achieved with measurements made on both experimental models at 10.900 GHz (311.4 MHz). The results are given in figure 9 where a comparison with theory is given. Computed radiation patterns for cases 1 to 3 over the range of 5.250 to 13.125 GHz (150 to 375 MHz) are presented in figure 10.

Pitch-Plane Radiation Patterns

Computations of the pitch-plane patterns (case 4) are more difficult, since the perimeter of the pitch-plane cross-section profile varies roughly from 60 to 150 wavelengths over the desired frequency range. Under this condition, application of RIEF would require the solution of a minimum of 300 simultaneous equations, a number which leads to

excessive computer storage requirements. The profile electrical size would indicate GTD to be a more useful approach for this computation. Unfortunately, GTD is not easily applicable to this profile, since practical use of GTD is limited currently to profiles convex in shape.

However, since patterns are of interest primarily in the lit region and in the forward direction, the portion of the pitch-plane cross-section profile from the back of the cockpit to the tail may be ignored by closing the cross section, as indicated in figure 11. The result is a polygon described by 178 points, leading to a system of 178 simultaneous equations. (See table I.) A computed pitch-plane pattern for the geometry of figure 11 is given in figure 12, with experimental verification obtained from the three-dimensional model of figure 5.

DISCUSSION OF RESULTS

The reliability of computing principal-plane radiation patterns of thin annular slots mounted on a spacecraft, such as the Space Shuttle orbiter, by use of RIEF and the approximations made is enhanced by the excellent agreement between theory and experiment shown in figures 9 and 12. It is evident from figures 9, 10, and 12 that a null occurs in the lit region on the normal to the plane of the annular slot aperture, and that major lobes occur at roughly 60° on either side of the normal. This result is generally true for a thin annular slot of mean radius a mounted on a ground plane of infinite extent and having a value of $ka \leq 2$, pattern breakup occurring for larger values⁵ of ka . (See ref. 18, pp. 8-8 and 8-9.)

If the annular slot is located at A, figures 9 and 10(a) reveal that ground coverage is poor, especially in the shadow regions. An improvement in ground coverage is achieved, as indicated in figure 10(b), if the annular slot is located at B_1 (or B_2), but coverage is asymmetrical unless both locations and a switching arrangement are used. However, symmetry is achieved if the annular slots at B_1 and B_2 are excited simultaneously, as indicated in figure 10(c), but pattern breakup is evident, as is generally encountered for arrays of widely separated antennas on electrically large bodies. Obviously, excellent ground coverage would be achieved if an annular slot were located on the underside of the orbiter, but this location is undesirable because of the excessive heat anticipated during atmospheric reentry. Figure 10 reveals that not only is the ripple structure finer as the frequency is increased, but also the fields in the shadow region are relatively weaker; that is, shadow boundaries are more sharply defined. Finally, figure 12 reveals that desired forward direction coverage results if the annular slot is located at A.

⁵Maximum value of $ka = k(d_M/2)$ for the annular slot in this paper is 2.25 at a frequency of 400 MHz.

It was noted that for all cases the phase of the radiation field fluctuates through many cycles, particularly in the shadow regions, as either ϕ_r or ϕ_p is varied from 0° to 360° . This result is generally true for antennas on electrically large bodies.

CONCLUDING REMARKS

In this paper, a digital computer program based on a two-dimensional integral equation formulation (Richmond Integral Equation Formulation) was applied to predict radiation patterns of annular slot antennas mounted on the Space Shuttle orbiter. The excellent agreement between computed patterns and patterns obtained from measurements made on 1/35-scale models supports the use of this approach for future similar spacecraft or aircraft antenna design problems.

By use of the Richmond Integral Equation Formulation, additional radiation patterns may be predicted easily as the design parameters of the orbiter or antenna are changed; thus, it is insured that proper radiation pattern coverage is maintained from design to construction. The Richmond Integral Equation Formulation may also be readily applied to predict patterns of other antennas of interest such as slot antennas. If antenna arrays are considered, the solution to the set of simultaneous equations automatically includes mutual coupling effects.

Although limited by computer storage requirements, the Richmond Integral Equation Formulation is characterized by ease of input data points describing the profile and antenna to be analyzed. In contrast, the use of geometrical theory of diffraction requires a much more critical selection of input data points and equations describing the body surface between any successive pair of points, since smooth functions of the radius of curvature and its arc length derivatives are required.

Langley Research Center,
National Aeronautics and Space Administration,
Hampton, Va., March 25, 1974.

APPENDIX A

DIGITAL COMPUTER PROGRAMS

The purpose of this appendix is to present and to describe the use of the digital computer programs employed to obtain computations and plots of the radiation patterns for the Space Shuttle annular slot antennas described in the text. As indicated in the text, the pattern computations and plots obtained by use of RIEF (see fig. 2) require a knowledge of (a) the X- and Y-coordinates of the end points of the segments used to approximate the cross-sectional profile of the orbiter in the plane in which the pattern is to be computed, and (b) the voltage strengths and the point indices of the equivalent narrow axial slot antennas representing the annular slot antennas. It should be noted in figure 2 that the end points of the profile segments are indexed in a counterclockwise direction, the first point being located at $\phi = 0^\circ$.

It is also indicated in the text that only a coarse number of points are specified initially and that the remaining points are generated with the aid of a spline fit procedure. In this appendix and in appendix B, for the sake of nomenclature, an initially specified point is designated as a "coarse point," and the index of the coarse point as the "coarse point index." Any one of the end points generated by the spline curve fit procedure and required for the computation of a radiation pattern is designated as an "actual point" and the index as the "actual point index."

The N' coarse points are defined and are indexed in the same manner as the N actual points defined in figure 2. However, coarse point N' is located and specified at the same point as coarse point 1. After the spline fit procedure is applied to generate the N actual points from specification of the coarse points, it will be found that the actual points consist of all the coarse points (except coarse point N') and additional points located between any two consecutive coarse points. If it is desired that the coarse points and the actual points be identical, then $N' = N + 1$. Under this condition, no points are generated between any pair of consecutive coarse points. If the spline fit procedure is used to generate additional points, however, then $N' \leq N + 1$.

The main program and all supporting subroutines used for analysis of the Space Shuttle annular slot antennas are given at the end of this appendix. This program requires a specification of the following data: (a) number of coarse points N' and the X- and Y-coordinates of each coarse point, (b) the indices of the coarse points at which the equivalent narrow axial slots are located,⁶ (c) the voltage strengths of the narrow axial slots,

⁶A narrow axial slot is required to be located at a coarse point; conversely, a coarse point is required to be designated at a narrow axial slot.

APPENDIX A - Continued

(d) the initial frequency, the incremental frequency, and the final frequency of the frequency range over which radiation patterns are to be computed, (e) an array of integers which indicate the number of segments that are to be generated between any two consecutive coarse points by means of a two-dimensional spline fit method, and (f) the coarse point index at which the spline fit is to be initiated.⁷

After these data are specified, the main program calls subroutine SPLFIT, which, in turn, calls subroutine SPFIT2, to generate the X- and Y-coordinates of the N actual points from the spline fit procedure. The main program then calls subroutine CVRTV to convert the coarse point indices of the narrow axial slots to the actual point indices as defined in figure 2. After calls to subroutines SPLFIT and CVRTV are made, then the main program, as a function of frequency, converts the X- and Y-coordinates of the N actual points from units of centimeters to units of wavelength and calls subroutine TESLOT to compute the radiation pattern.

Subroutine SKETCH is a subroutine which generates instructions on a magnetic tape used to drive the CalComp (California Computer Products, Inc.) plotter. Called by the main program, subroutine SKETCH plots the set of N actual points describing the cross-section profile. A call to subroutine SKETCH produces a plot similar to the plots given in figures 6 to 8, and immediately below the plot a scale is given. For the first call to subroutine SKETCH, the X- and Y-coordinates are in centimeters, and the scale is in centimeters per inch (on the plotting paper). For the remaining calls to subroutine SKETCH, the X- and Y-coordinates are in wavelengths, and the scale is in wavelengths per inch (on the plotting paper).

Subroutine DBPLOT is a subroutine also used to generate instructions on a magnetic tape for driving the CalComp plotter. At each frequency over the range of frequencies for which a radiation pattern is desired, subroutine DBPLOT produces a polar plot of radiation field magnitude, in decibels, against ϕ_p or ϕ_r and a rectangular plot of radiation field phase, in degrees, against ϕ_p or ϕ_r .

The programs given apply for obtaining computations and plots of radiation patterns of, in general, a set of narrow axial slot antennas (or annular slot antennas, each of which is represented by a pair of narrow axial slots) mounted on a cylinder of arbitrary cross section. In order to use the programs, the user is required to have additional knowledge of how the input data are set up for transmission to the main program and to have a knowledge of how the arrays in the main program are dimensioned.

⁷The point at which the spline fit is initiated is chosen to be in an approximately linear region of the profile.

APPENDIX A – Continued

Input Data

All input data are read in through the main program. The first input data card contains the following quantities: NPTIN, ISTART, NPORD, MADM, KI, KWRT1, KWRT2, KWRT3, ISKIPP, ISIZEP, HPAT, FMCO, FMCD, and FMCF. The quantities are defined as follows:

NPTIN	Number of coarse points describing the cross-section profile (NPTIN \leq N + 1, where N = Actual number of points, as defined in fig. 2)
ISTART	Coarse point index at which the spline fit is to be initiated (1 \leq ISTART \leq NPTIN)
NPORD	Number of narrow axial slots (1 \leq NPORD \leq NPTIN)
MADM	1 or 0. For MADM = 1, the short-circuit admittance matrix for all ports (that is, narrow axial slots) is computed. For MADM = 0, this computation is avoided. (In this paper, MADM = 0 for all computations)
KI	number of angular values of ϕ_p or ϕ_r at which the radiation field E_ϕ is computed (KI = 361, which is used for all computations in this paper, gives pattern computations in 10^0 increments)
KWRT1	1 or 0. KWRT1 = 1 gives a write out of the X- and Y-coordinates, in wavelengths, of the N actual points and the distance, in wavelengths, between any two consecutive segments. KWRT1 = 0 avoids this write out
KWRT2	1 or 0. KWRT2 = 1 gives a write out of the real part, the imaginary part, the magnitude, and the phase of the radiation field E_ϕ for each of the KI angular values of ϕ_p or ϕ_r . KWRT2 = 0 avoids this write out
KWRT3	1 or 0. KWRT3 = 1 gives a write out of the value of E_ϕ in decibels, the normalized value of E_ϕ , and the phase of the radiation field E_ϕ for each of the KI angular values of ϕ_p or ϕ_r . The value of E_ϕ in decibels and the normalized value of E_ϕ are with respect to the maximum value of E_ϕ occurring among the KI values of E_ϕ computed. KWRT3 = 0 avoids this write out
ISKIPP	Integer required for obtaining radiation pattern plots. ISKIPP is positive for line and symbol plots, and is negative for symbol-only plots. The magnitude of ISKIPP specifies the alternate number of data points at which a symbol is plotted

APPENDIX A - Continued

ISIZEP	1, 2, or 3. ISIZEP = 1 produces small size symbols, ISIZEP = 2 produces medium size symbols, and ISIZEP = 3 produces large size symbols
HPAT	A floating point number that is five times the radius, in inches, of the polar plots to be made with subroutine DBPLOT.
FMCO	Initial frequency, in MHz, for which pattern computations are to be made
FMCD	Incremental frequency, in MHz, for which pattern computations are to be made
FMCF	Final frequency, in MHz, for which pattern computations are to be made

After the first data card is read in, a set of NPORT data cards is then read into the main program. On each card are specified the port index I, the coarse point index JVGS(I), and the complex voltage strength VGS(I) of the Ith port (that is, the Ith narrow axial slot).

Next, a set of NPTIN data cards is read into the main program. On each card is an identifying integer IGNORE, the X-coordinate PNTIN (I,1), in cm, and the Y-coordinate PNTIN (I,2), in cm, of the Ith coarse point.

Finally, the IDIVD array of integers is read into the main program. The IDIVD array of integers is a set of NSEG = (NPTIN - 1) integers INDIVD(I) (I = 1, 2, . . . , NSEG) which specify the number of segments that will occur between any pair of consecutive coarse points as a result of the use of subroutines SPLFIT and SPFIT2. Specifically, if IDIVD(I) = IX, then IX segments will occur (or IX-1 points will be generated) between coarse point I and coarse point I + 1. All segments between any two consecutive coarse points are approximately equal in length, which should be no greater than $\lambda/4$ at the highest frequency for which radiation pattern computations are desired. It should be noted that the sum of the NSEG integers in the IDIVD array is equal to the number of actual segments and points N generated for use in subroutine TESLOT. As noted in the text, this number should not exceed 180 if the Control Data Corporation 6600 computer at NASA Langley Research Center is employed. If the generation of spline-fitted points is desired to be avoided altogether (that is, the coarse points and the actual points are identical, except that coarse point N' is omitted), it is necessary only to set all NSEG integers equal to 1 in the IDIVD array. Under this condition, the N + 1 coarse points become the N points required by subroutine TESLOT for computation of the radiation pattern.

Dimension of Arrays in the Main Program

In some applications, the user may wish to change the dimensions of the arrays in the main program. To change the dimensions, define the following integers:

APPENDIX A – Continued

n_1 maximum number of actual points (and simultaneous equations)
 n_2 maximum number of narrow axial slots
 n_3 maximum number of angular values for which radiation patterns are desired
 $n_4 \geq n_3 + 2$
 n_5 maximum number of coarse points

Then the following statements must appear in the main program:

```
PROGRAM MAIN (INPUT, OUTPUT, . . .)
COMMON/BLK1/KNTPLT, XNEW, YNEW
COMPLEX VGS, C, CJ, EPP, YMMHO, ZINPUT
DIMENSION X( $n_1$ ), Y( $n_1$ ), XC( $n_1$ ), YC( $n_1$ ), VGS( $n_2$ ), IVGS( $n_2$ ),
1 D( $n_1$ ), C( $n_1, n_1$ ), CJ( $n_1$ ), EPP( $n_1$ ), YMMHO( $n_2, n_2$ ),
2 THTA( $n_4$ ), AEPEH1( $n_4$ ), RATIO( $n_4$ ), PEPH1( $n_4$ ), AEY( $n_4$ ),
3 XW( $n_1$ ), YW( $n_1$ ), PNTIN( $n_5, 2$ ), SPNTIN( $n_5, 2$ ), IDIVD( $n_5$ ),
4 ELEN( $n_5$ ), COEF( $n_5, 4, 2$ ), XPNT( $n_1$ ), YPNT( $n_1$ ), JVGS( $n_2$ )
MAXP =  $n_5$ 
MAXCO =  $n_5$ 
MXNPT =  $n_1$ 
MXPORT =  $n_2$ 
CALL CALCOMP
CALL LEROY
KNTPLT = 0
.
.
.
END
```

APPENDIX A - Continued

For the main program n_1 corresponds to 170, n_2 to 4, n_3 to 723, n_4 to 725, and n_5 to 57. A restriction is that the sum of the NSEG integers in the IDIVD array must not exceed the value of n_1 .

Main Computer Program for Obtaining Computations of Space

Shuttle Annular Slot Antenna Radiation Patterns

```

PROGRAM MAIN(INPUT,OUTPUT,TAPE5=INPUT,TAPE6=OUTPUT)
J. EARL JONES, ARS-TRB-FIL, PHONE 3E31, MAIL STOP 490--NASA45897C
C
C ***** ****
C *
C * PURPOSE - TO SET UP INPUT DATA TO SUBROUTINES TESLOT AND CBPLOT *
C * TO OBTAIN, OVER A RANGE OF FREQUENCIES, RADIATION *
C * PATTERN CALCULATIONS AND PLOTS AND TO OBTAIN THE *
C * SHORT CIRCUIT ADMITTANCE MATRIX OF AN ARRAY OF TE *
C * SLOTS ON A PERFECTLY CONDUCTING CYLINDER OF ARBITRARY *
C * CROSS SECTION *
C *
C * DEFINITIONS  FMCO=INITIAL FREQUENCY, MHZ. *
C * FMCD=INCREMENTAL FREQUENCY, MHZ. *
C * FMCF=FINAL FREQUENCY, MHZ. *
C *
C * NPOINT,MNPT,NPORT,MXPRT,MAUD,MK,KWRT1,KWRT2,
C * KWRT3,VGS,IVGS,XW,YW,THTA,AEPH1,RATIC,PEPH1,YMMHO,
C * ZINPUT, AND LPTEPH ARE DEFINED IN SUBROUTINE *
C * TESLOT. ISKIPP,ISIZEP,AND HPAT ARE DEFINED IN *
C * SUBROUTINE CBPLOT. *
C *
C * IF ANALYSIS OCCURS OVER A RANGE OF FREQUENCIES,
C * VALUES IN XW AND YW ARE INITIALLY READ IN IN CM.
C * AND THESE VALUES ARE STORED IN XC AND YC ARRAYS.
C * IF EITHER FMCL, FMCO, OR FMCF ARE SET TO A
C * NEGATIVE VALUE, THEN VALUES IN XW AND YW ARE
C * UNDERSTOOD TO BE READ IN IN WAVELENGTHS.
C *
C ***** ****
C
C COMMON /HLK1/ KNTPLT,XNEW,YNEW
C COMPLEX VGS,C,CJ,EPP,YMMHO,ZINPUT
C DIMENSION X(170),Y(170),XC(170),YC(170),VGS(4),IVGS(4),
C 1 U(170),C(170,170),CJ(170),EPP(170),YMMHC(4,4),
C 2 THTA(725),AEPH1(725),RATIC(725),PEPH1(725),AEY(725),
C 3 XW(170),YW(170),PNTIN(57,2),SPNTIN(57,2),IDIVD(57),
C 4 ELEN(57),COEF(57,4,2),XPNT(170),YFNT(170),JVGS(4)
C
C MAP=57
C MAXCO=57
C MNPT=170
C MXPRT=4
C CALL CALCOMP
C CALL LEROY
C KNTPLT=0
C KTV=1
C 1 READ(5,101) NPTIN,ISTART,NPUKT,MAUD,MK,KWPT1,KWRT2,KWRT3,
C 1 ISKIPP,ISIZEP,HPAT,FMCO,FMCU,FMCF
C 1 IF(EUF,5) 4,6
C 4 IF(KNTPLT.EQ.0) GO TO 5
C 4 CALL CALPLT(XNEW,YNEW,-999)
C 5 STOP

```

APPENDIX A - Continued

```

6 CONTINUE
IF((FMCO.LE.0.) .OR. (FMCU.LE.0.) .OR. (FMCF.LE.0.)) KTV=0
READ(5,103) (I,JVGS(I)),VGS(I),I=1,NPORT
READ(5,104) (IGNORE,PNTIN(I,1),PNTIN(I,2),I=1,NPTIN)
NSEG=NPTIN-1
READ(5,108) (IDIVD(I),I=1,NSEG)
CALL SPLFIT(MAXP,MAXCC,NPTIN,ISTART,PNTIN,IDLVD,ELEN,
1 COEF,SPNTIN,XPNT,YPNT,NPCINT,XW,YW)

1
1
1

CALL CVRTV(NPTIN,NPORT,JVGS,IDLVD,IVGS)
WRITE(6,200)
WRITE(6,204) NPTIN,ISTART
WRITE(6,208)
WRITE(6,206)
WRITE(6,108) (IDLVD(I),I=1,NSEG)
WRITE(6,208)
WRITE(6,201)
WRITE(6,151) NPCINT,MANPT,NPCRT,MXPRT,MACM,KI,KWRT1,
1 KWRT2,KWRT3,ISKIPP,ISIZEP,HPAT,FMCO,FMCU,FMCF
WRITE(6,208)
IF(KTV.EQ.0) IUNITS=2
IF(KTV.EQ.1) IUNITS=1
CALL SKETCH(XW,YW,NPOINT,HPAT,1,22,1,IUNITS)
IF(KTV.EQ.0) GO TO 14
DO 10 I=1,NPOINT
XC(I)=XW(I)
YC(I)=YW(I)
10 CONTINUE
WRITE(6,209)
WRITE(6,210)
WRITE(6,152) (I,XC(I),YC(I),I=1,NPOINT)
WRITE(6,206)
WRITE(6,202)
FMC=FMCO

11 WVL=30000./FMC
WRITE(6,211) FMC,WVL
DO 12 I=1,NPOINT
XW(I)=XC(I)/WVL
YW(I)=YC(I)/WVL
12 CONTINUE
WRITE(6,208)
CALL SKETCH(XW,YW,NPOINT,HPAT,1,22,1,2)
14 CONTINUE
CALL TESLOT(NPCINT,MANPT,NPORT,MXPRT,MACM,KI,
1 KWRT1,KWRT2,KWRT3,
2 XW,YW,VGS,X,Y,L,C,CJ,EFF,THTA,AEPH1,RATIO,PEPH1,
3 YMHC,ZINPUT,LPTEPH)
IF(LPTEPH.EQ.0) GO TO 18
CALL DRPLT(HPAT,KI,ISKIPP,ISIZEP,THTA,AEPH1,AEY,PEPH1)
GO TO 20
18 WRITE(6,224) LPTEPH
20 CONTINUE
WRITE(6,206)
WRITE(6,218)
WRITE(6,219)
DO 24 I=1,NPORT
DO 24 J=1,NPCRT
ISCRPT=IVGS(I)
JSCRPT=IVGS(J)
WRITE(6,154) ISCRPT,I,JSCRPT,J,YMHC(I,J)
24 CONTINUE
IF(NPORT.GT.1) GO TO 28
WRITE(6,208)
WRITE(6,222) ZINPUT

```

APPENDIX A - Continued

```

28 IF(KTV.EQ.0) GO TO 1
FMC=FMCO+FMCD
WRITE(6,202)
IF(FMC.LE.FMCF) GO TO 11
GO TO 1
101 FORMAT(10I5,F5.0,3F7.0)
103 FORMAT(2I5,2F10.0)
104 FORMAT(I5,2F10.0)
108 FORMAT(40I2)
151 FORMAT(11I7,F7.2,3F7.1)
152 FORMAT(1I10,2F15.4)
154 FORMAT(1I12,3I7,2F16.8)
200 FORMAT(1I0H ****,*****)
201 FORMAT(105H NPOINT MXNPT NPRT MPORT MADM KI KWRT1 KWRT
12 KWRT3 ISKIPP ISIZEP HPAT FMCO FMCD FMCF)
202 FORMAT(1I0H -----,/)
204 FORMAT(1X,6HNPTIN=I2,3X,7HISTART=I2,/)
206 FORMAT(1X,18HIUIVD ARRAY VALUES,/)
208 FORMAT(/)
209 FORMAT(13X,1BHLCCATION OF PCINTS)
210 FORMAT(5X,35HPCINT X, CM. Y, CM.,/)
211 FORMAT(5X,10HFREQUENCY=F7.1,4H MHZ/,5X,11HWAVELENGTH=F7.2,4H CM.)
218 FORMAT(5X,31HSHCRT-CIRCUIT ADMITTANCE MATRIX,/)
219 FORMAT(5X,60H PCINT PORT POINT PORT G, MILLIMHOS B, MI
1LLIMHOS)
222 FORMAT(5X,8HZINPUT=(F16.8,1H,F16.8,6H) CHMS,/)
224 FORMAT(5X,7HLPTEPH=I2,14H FOR THIS CASE,/)
END

```

Subroutine TESLOT

```

SUBROUTINE TESLOT(NPOINT,MXNPT,NPORT,MPORT,MADM,KI,
1 KWRT1,KWRT2,KWRT3,
2 XN,YN,VGS,IVGS,X,Y,D,C,CJ,EPP,THTA,AEPH1,RATIO,PEPH1,
3 YMMHO,ZINPUT,LPTEPH)

```

```

*****
*
* PURPOSE TO CALCULATE THE RADIATION PATTERN AND TO CALCULATE *
* THE SHORT CIRCUIT ADMITTANCE MATRIX OF AN ARRAY OF TE *
* SLGT ANTENNAS LOCATED ON A PERFECTLY CONDUCTING *
* CYLINDER OF ARBITRARY CROSS SECTION *
*
* INPUT DATA NPOINT=NUMBER OF POINTS DESCRIBING THE CYLINDER *
* MXNPT=MAXIMUM PERMISSIBLE NUMBER OF POINTS *
* NPORT=NUMBER OF SLOT ANTENNAS IN THE ARRAY *
* MPORT=MAXIMUM PERMISSIBLE NUMBER OF SLOT ANTENNAS *
* MADM=1 IF SHCRT CIRCUIT ADMITTANCE MATRIX IS TO BE *
* COMPUTED, 0 FOR NO COMPUTATIONS. MATRIX IS *
* ALWAYS COMPUTED IF NPORT=1, HOWEVER. *
* KI=NUMBER OF RADIATION PATTERN POINTS TO BE COMPUTED/ PLUTTED PER CASE. FOR 5 DEG. INCREMENTS *
* SET KI=72+1, FOR 4 DEG. INCREMENTS SET KI=90+1, *
* FOR 3 DEG. INCREMENTS SET KI=120+1, ETC. *
* KWRT1=1 FOR WRITEOUT OF ARRAY OF POINT LOCATIONS, *
* AND ARRAY OF SLOT ANTENNA LOCATIONS, *
* 0 FOR NO WRITEOUT *
* KWRT2=1 FOR WRITEOUT OF RELATIVE RADIATION PATTERN, *
* 0 FOR NO WRITEOUT

```

APPENDIX A - Continued

```

C      *      KWRTG=1 FOR WRITEOUT OF DB RADIATION PATTERN,      *
C      *      0 FOR NO WRITEDOUT      *
C      *      XW=ARRAY OF X-VALUES OF COORDINATES, WAVELENGTHS      *
C      *      YW=ARRAY OF Y-VALUES OF COORDINATES, WAVELENGTHS      *
C      *      VGS=ARRAY OF VALUES OF SLOT VOLTAGES      *
C      *      IVGS=ARRAY OF VALUES OF THE LOCATIONS (CORRESPONDING      *
C      *      TO THOSE IN THE XW AND YW ARRAYS) OF THE      *
C      *      SLCT VOLTAGES IN THE VGS ARRAY      *
C      *
C      *      OUTPUT DATA      THTA=ARRAY CONTAINING THE ANGULAR VALUES      *
C      *      (DEGREES) FOR WHICH THE RADIATION FIELD IS      *
C      *      TO BE PLOTTED.      THTA(1)=0., THTA(KI)=360.      *
C      *      AEPH1=ARRAY OF MAGNITUDE VALUES (DB) CORRESPONDING      *
C      *      TO ANGULAR VALUES IN THTA ARRAY      *
C      *      RATIO=ARRAY OF VALUES OF (E/EMAX) CORRESPONDING      *
C      *      TO ANGULAR VALUES IN THTA ARRAY      *
C      *      PEPH1=ARRAY OF PHASE VALUES (DEGREES)      *
C      *      CORRESPONDING TO ANGULAR VALUES IN THTA      *
C      *      ARRAY      *
C      *      YMMDHO=SHORT CIRCUIT ADMITTANCE MATRIX, MILLIMHOS      *
C      *      ZINPUT=INPUT IMPEDANCE, OHMS (ONLY FOR NP3RT=1)      *
C      *      LPTEPH=1 INDICATES A RADIATION FIELD PLOT FOR USE      *
C      *      IN DBPLOT WAS COMPUTED, 0 INDICATES THERE      *
C      *      WAS NO RADIATED FIELD, AND HENCE NO PLOT      *
C      *      WAS COMPUTED      *
C      *
C      *      X,Y,U,C,CJ,EPP ARE ARRAYS USED FOR INTERMEDIATE CALCULATIONS      *
C      *
C      *      RESTRICTIONS      IN CALLING PROGRAM, VGS,C,CJ,EPP,YMMHD,AND ZINPUT*      *
C      *      MUST BE TYPED COMPLEX.      ARRAYS XW,YW,X,Y,U,EPP,      *
C      *      AND CJ MUST BE DIMENSIONED WITH THE VALUE OF      *
C      *      MXPNT AND C MUST BE DIMENSIONED AS C(MXPNT,MXPNT)*      *
C      *      IN CALLING PROGRAM.      ARRAYS VGS AND IVGS MUST      *
C      *      BE DIMENSIONED WITH THE VALUE OF MPORT AND YMMDHO*      *
C      *      MUST BE DIMENSIONED AS YMMDHO(MXPCRT,MXPORT) IN      *
C      *      CALLING PROGRAM.      FOR PLOT PURPOSES, ARRAYS THTA,*      *
C      *      AEPH1,RATIO, AND PEPH1 MUST BE DIMENSIONED AT      *
C      *      LEAST AS LARGE AS THE VALUE (KI+2) IN CALLING      *
C      *      PROGRAM.      *
C      *
C      ****
CCOMPLEX VGS,YMMHD,CJ,C,EPP,CUT,EPS,ZINPLT
COMPLEX P11,P12,C11,W12,Q21,W22,EP1,EP2
DIMENSION X(1),Y(1),U(1),VGS(1),IVGS(1),C(MXNPT,1),
1 CJ(1),YMMHD(MXPCRT,1),EPP(1),AEPH1(1),RATIO(1),PEPH1(1),
2 THTA(1), XW(1),YW(1)
N=NPOINT
1DM=MXNPT
INT=10
CMAX=1.E-12
SWT2=SQRT(2.)
PI=3.141592653589793
TP=2.*PI
RDN=PI/180.
ETA=376.727
CWT=-2.*SWT2/(ETA*(1.,1.))
ZINPUT=CMPLX(0.,C.)
DO 20 I=1,N
IP=I+1
IFI(I.EQ.N) IP=1
DX=XW(IP)-XW(I)
DY=YW(IP)-YW(I)
D(I)=SQRT(DX*DX+DY*DY)

```

APPENDIX A – Continued

```

20 CONTINUE
IF(KWRT1.EQ.0) GO TO 804
  WRITE(6,601)
  WRITE(6,701) N
  WRITE(6,601)
  WRITE(6,702)
  WRITE(6,703)
  WRITE(6,601)
  DO 804 I=1,N
  DO 801 J=1,NPORT
    ISCRPT=IVGS(J)
    IF(ISCRPT.EQ.1) GO TO 802
 801 CONTINUE
    WRITE(6,603) I,XW(I),YW(I),U(I)
    GO TO 803
 802 WRITE(6,604) I,XW(I),YW(I),U(I),VGS(J)
 803 IF(I.LT.N) GO TO 804
    WRITE(6,601)
 804 CONTINUE
    DO 22 I=1,N
      X(I)=TP*XW(I)
      Y(I)=TP*YW(I)
      U(I)=TP*U(I)
 22 CONTINUE
    DO 25 I=1,NPORT
      DC 25 J=1,NPORT
      YMMHO(I,J)=(0.,0.)
 25 CONTINUE
    DO 100 I=1,N
      DO 100 J=1,N
        C(I,J)=(0.,0.)
 100 CONTINUE
    DO 150 I=1,N
      CALL SMM1(U(I),P11,P12)
      C(I,I)=C(I,I)+P11
      J=I+1
      IF(I.EQ.N)J=1
      C(J,J)=C(J,J)+P11
      C(I,J)=C(I,J)+P12
      C(J,I)=C(J,I)+P12
 150 CONTINUE
    DO 200 I=1,N
      I=I
      IM=I-1
      IF(I.EQ.1)IM=N
      IP=I+1
      IF(I.EQ.N)IP=1
      U=U(I)
      UM=U(IM)
      CALL SMM2(X(IM),Y(IM),X(I),Y(I),X(IP),Y(IP),DM,DI,
      2INT,Q11,Q12,Q21,Q22)
      C(I,I)=C(I,I)+Q21
      C(IM,I)=C(IM,I)+Q11
      C(IM,IP)=C(IM,IP)+Q12
      C(I,IP)=C(I,IP)+Q22
      DK=(UM+DI)/2.
      DUD=100.*ABS(DI-UM)/DK
      IF(DUD.LT.3.1GO TO 160
      CALL ZMM2(X(IP),Y(IP),X(I),Y(I),X(IM),Y(IM),DI,DM,
      2INT,Q11,Q12,Q21,Q22)
 160 CONTINUE
      C(I,I)=C(I,I)+Q21
      C(I,IM)=C(I,IM)+Q22
      C(IP,I)=C(IP,I)+Q11
      C(IP,IM)=C(IP,IM)+Q12

```

APPENDIX A – Continued

```

200 CONTINUE
  IF(N.LT.4) GO TO 260
  N1=N-1
  N2=N-2
  N4=N-4
  DO 250 J=1,N1
    I=J+1
    IF(J.EQ.1) I=N
    PI=I
    DI=D(I)
    X1=X(I)
    Y1=Y(I)
    X2=X(J)
    Y2=Y(J)
    KA=J+1
    KB=KA+N4
    DO 240 K=KA,KB
      IF(K.GT.N) GO TO 240
      FK=K
      DK=D(K)
      X3=X(K)
      Y3=Y(K)
      L=K+1
      IF(L.EQ.N) L=1
      X4=X(L)
      Y4=Y(L)
      CALL SMM3(X1,Y1,X2,Y2,X3,Y3,X4,Y4,DI,DK,Q11,Q12,Q21,Q22)
      C(I,K)=C(I,K)+Q11
      C(J,L)=C(J,L)+Q22
      C(I,L)=C(I,L)+Q12
      C(J,K)=C(J,K)+Q21
  240 CONTINUE
  250 CONTINUE
  260 CONTINUE
  KLCRT=0
  IF((MAUM.EQ.0).OR.(NPORT.EQ.1)) GO TO 268
  NAD=1
  DO 283 JJX=1,NPCRT
    KLCRT=KLCRT+1
    ISCRPT=IVGS(JJX)
    DO 265 I=1,N
      CJ(I)=(0.,0.)
  265 CONTINUE
  CJ(ISCRPT)=-VGS(JJX)
  GO TO 275
  268 NAD=0
  KLCRT=KLCRT+1
  DO 271 I=1,N
    CJ(I)=(0.,0.)
  271 CONTINUE
  DO 274 I=1,NPORT
    ISCRPT=IVGS(I)
    CJ(ISCRPT)=-VGS(I)
  274 CONTINUE
  275 IF(KLCRT.GT.1) GO TO 277
    CALL CROUT1(C,CJ,N,IDM,0,0)
    GO TO 280
  277 CALL CRCUT2(C,CJ,N,IDM,0,0)
  280 IF(NAD.EQ.0) GO TO 286
    DO 283 JJY=1,NPCRT
      JSRPT=IVGS(JJY)
      YMMLH0(JJY,JJX)=1000.* (CJ(JSRPT)/VGS(ISCRPT))
  283 CONTINUE
  GO TO 268
  286 IF(NPORT.GT.1) GO TO 289
    YMMLH0(1,1)=1000.* (CJ(ISCRPT)/VGS(ISCRPT))
    ZINPUT=CMPLX(1000.,0.)/YMMLH0(1,1)

```

APPENDIX A – Continued

```

289 CONTINUE
  KIM=KI-1
  DPH=360./FLOAT(KIM)
  AEPHMX=0.
  DO 390 NPH=1,KI
    FPH=NPH-1
    PHS=JPH*FPH
    THTA(NPH)=PHS
    PHR=.0174533*PHS
    CPH=COS(PHR)
    SPH=SIN(PHR)
    DO 300 I=1,N
      EPP(I)=(.0,.0)
300 CONTINUE
  DO 350 I=1,N
    XA=X(I)
    YA=Y(I)
    IP=I+1
    IF(I.EQ.N)IP=1
    XB=X(IP)
    YB=Y(IP)
    DU=U(I)
    CALL CFF(XA,YA,AE,YB,CL,CPH,SPH,EP1,EP2)
    EPP(I)=EPP(I)+EP1
    EPP(IP)=EPP(IP)+EP2
350 CONTINUE
  EPS=(.0,.0)
  DO 384 I=1,N
    EPS=EPS+CJ(I)*EPP(I)
384 CONTINUE
  EPAB=CABS(EPS)
  IF(EPAB.GE.AEPHMX) AEPHMX=EPAB
  AEPH1(NPH)=EPAB
  REPS=REAL(EPS)
  XEPS=AIMAG(EPS)
  IF(EPAB.LE.CMAX) GO TO 385
  PEPH1(NPH)=ATAN2(XEPS,REPS)/RDN
  GO TO 387
385 PEPH1(NPH)=0.
387 CONTINUE
  IF(KWRT2.EQ.0) GO TO 390
    IF(NPH.GT.1) GO TO 388
    WRITE(S,601)
    WRITE(S,710)
    WRITE(S,601)
    WRITE(S,711)
    WRITE(S,601)
388 WRITE(S,605) THTA(NPH),REPS,XEPS,EPAB,PEPH1(NPH)
    IF(NPH.LT.KI) GO TO 390
    WRITE(S,601)
390 CONTINUE
  LPTEPH=1
  IF(AEPHMX.LE.CMAX) GU TO 425
  DO 424 KL=1,KI
    AEPH2=AEPH1(KL)
    ALPH=AEPH2/AEPHMX
    RATIO(KL)=ALPH
    IF(ALPH.LE.CMAX) GO TO 423
    ALPHD8=20.*ALOG10(ALPH)
    IF(ALPHD8.LE.-40.) GO TO 423
    AEPH1(KL)=ALPHD8
    GO TO 424
423 AEPH1(KL)=-40.
424 CONTINUE
  GU TO 426

```

APPENDIX A - Continued

```

425 LPTEPH=0
426 CONTINUE
1F(LPTEPH.EQ.0) GO TO 475
1F(KWRT3.EQ.0) GO TO 485
    WRITE(6,601)
    WRITE(6,714)
    WRITE(6,601)
    WRITE(6,715)
    WRITE(6,601)
    DO 430 KL=1,KI
    WRITE(6,608) THTA(KL),AEPHI(KL),RATIO(KL),PEPHI(KL)
    IF(KL.LT.KI) GO TO 430
    WRITE(6,602)
430 CONTINUE
    RETURN
475 WRITE(6,718) AEPHMX
485 CONTINUE
    RETURN
601 FORMAT(/)
602 FORMAT(//)
603 FORMAT(19,3F11.4)
604 FORMAT(19,3F11.4,F20.4,F15.4)
605 FORMAT(F14.1,3E15.6,F15.2)
608 FORMAT(F14.1,2F15.6,F15.2)
701 FORMAT(5X,41HNUMBER OF POINTS DESCRIBING THE CYLINDER=I3)
702 FORMAT(5X,37HGECMETRY OF CYLINDRICAL CROSS SECTION,9X,22HDRIVING P
1CINT VOLTAGES)
703 FORMAT(4X,38HPOINT X, WVL. Y, WVL. U, WVL.,5X,30H RE(V)
1, VOLTS IM(V), VOLTS)
710 FORMAT(5X,29HRADIATION PATTERN (RELATIVE))
711 FORMAT(5X, 9RPHI, DEG.,8X,7HRE(EPH),8X,7HIM(EPH),7X,8HMAG(EPH),4X,
1 11HPHASE, DEG.)
714 FORMAT(5X,35HRADIATION PATTERN (DB AND E/EMAX))
715 FORMAT(5X,9RPHI, DEG.,7X,8HEPH, DB.,9X,6HE/EMAX,4X,
2 11HPHASE, DEG.)
718 FORMAT(5X,7HAEPHMX=E15.8,34H, THUS, NO CB VALUES WERE COMPUTED)
    END

```

Subroutine SPLFIT

```

SUBROUTINE SPLFIT(MAXP,MAXCC,NPTIN,ISTART,PNTIN,IOIVD,
1 ELEN,COEF,SPNTIN,XPNT,YPNT,APCINT,XW,YW)
DIMENSION PNTIN(MAXP,2),SPNTIN(MAXP,2),COEF(MAXCC,4,2),
1 ELEN(1),IOIVD(1),XPNT(1),YPNT(1),XW(1),YW(1)
NSEG=NPTIN-1
DO 10 I=1,NPTIN
K=(ISTART-1)+I
IF(K.LE.NPTIN) GO TO 9
K=(ISTART-NPTIN)+I
9 SPNTIN(I,1)=PNTIN(K,1)
SPNTIN(I,2)=PNTIN(K,2)
10 CONTINUE
CALL SPFIT2(MAXP,MAXCC,NPTIN,SPNTIN,COEF,ELEN)
IV=1
DO 17 I=1,NSEG
IVK=(ISTART-1)+I
IF(IVK.LE.NSEG) GO TO 14
IVK=(ISTART-NSEG)+I-1
14 ICV=IOIVD(IVK)
DO 17 J=1,IVD
JM1=J-1
T=(FLOAT(JM1)/FLOAT(IVD))*ELEN(I)
T2=T*T

```

APPENDIX A - Continued

```

T3=T*T2
XPNT(IV)=T3*CDEF(I,1,1)+T2*CDEF(I,2,1)+T*CDEF(I,3,1)+CDEF(I,4,1)
YPNT(IV)=T3*CDEF(I,1,2)+T2*CDEF(I,2,2)+T*CDEF(I,3,2)+CDEF(I,4,2)
IV=IV+1
17 CONTINUE
NPOINT=IV-1
LXX=I START-1
LXSUM=0
DO 19 I=1,LXX
LXSLM=LXSUM+IDIVE(I)
19 CONTINUE
DO 22 I=1,NPOINT
J=LXSUM+1
IF(J.GT.NPOINT) J=J-NPOINT
XW(J)=XPNT(I)
YW(J)=YPNT(I)
22 CONTINUE
RETURN
END

```

Subroutine SPFIT2

```

SUBROUTINE SPFIT2(MAXP,MAXCC,N,PNT,CDEF,ELEN)
C
C THIS SUBROUTINE COMPUTES THE PARAMETRIC CUBIC SPLINE COEFFICIENTS
C TO APPROXIMATE A SMOOTH CURVE THROUGH A 2D SET OF POINTS PNT(I,1)
C AND PNT(I,2). THE ARC LENGTH ELEN(I) IS APPROXIMATED TO BE
C THE EUCLIDEAN DISTANCE BETWEEN CONSECUTIVE POINTS
C
C MAXP=MAX. NUMBER OF INPUT POINTS ALLOWED
C MAXCC=MAX. NUMBER OF SPLINES ALLOWED
C N=ACTUAL NUMBER OF INPUT POINTS
C
C EXAMPLE-SUPPOSE 20 POINTS TO BE INPUT, CALLING PROGRAM HAS FOLLOWING
C DIMENSION PNT(50,2),CDEF(50,4,2),ELEN(50)
C THEN N=20, MAXP=50, MAXCC=50
C
C
C DIMENSION PNT(MAXP,2),CDEF(MAXCC,4,2),ELEN(1)
C NUNE=1
C N1=N-NUNE
C TWO=2.
C ONE=1.
C THREE=3.
C
C DO 10 I=1,N1
C IP=I+NUNE
C X1=PNT(IP,1)-PNT(1,1)
C Y1=PNT(IP,2)-PNT(1,2)
C ELL=X1*X1+Y1*Y1
C ELEN(I)=SQRT(ELL)
C 10 CONTINUE
C
C FORM A-MATRIX, SUPER DIAG. ELEMENTS ARE IN CDEF(I,4,1), SUB DIAG.
C ELEMENTS IN CDEF(I,2,1), DIAG. ELEMENTS IN CDEF(I,1,1), ELEMENTS
C OF COLUMN VECTOR FOR X EQUATION IN CDEF(I,3,1) AND Y EQUATION IN
C CDEF(I,3,2)
C
C CDEF(1,2,1)=0.
C CDEF(1,1,1)=TWO
C CDEF(1,4,1)=ONE
C CDEF(N,2,1)=CNE
C CDEF(N,4,1)=0.
C CDEF(N,1,1)=TWO

```

APPENDIX A - Continued

```

X1=THREE/ELEN(1)
Y1=THREE/ELEN(N1)
COEF(1,3,1)=X1*(PNT(2,1)-PNT(1,1))
COEF(1,3,2)=X1*(PNT(2,2)-PNT(1,2))
COEF(N,3,1)=Y1*(PNT(N,1)-PNT(N1,1))
COEF(N,3,2)=Y1*(PNT(N,2)-PNT(N1,2))
DO 20 I=2,N1
IM=I-NONE
IP=I+NONE
COEF(I,2,1)=ELEN(I)
COEF(I,1,1)=TWO*(ELEN(I)+ELEN(IM))
COEF(I,4,1)=ELEN(IM)
X1=THREE/(ELEN(I)*ELEN(IM))
X2=ELEN(IM)*ELEN(IM)
X3=ELEN(I)*ELEN(1)
COEF(I,3,1)=X1*(X2*(PNT(IP,1)-PNT(I,1))+X3*(PNT(I,1)-PNT(IM,1)))
COEF(I,3,2)=X1*(X2*(PNT(IP,2)-PNT(I,2))+X3*(PNT(I,2)-PNT(IM,2)))
20 CONTINUE
C
C      THE A-MATRIX IS TRIDIAGONAL, THE A-MATRIX WILL BE DECOMPOSED INTO
C      AN UPPER DIAG. MATRIX U AND A LOWER DIAG. MATRIX L SUCH THAT LU=A
C      THE DECOMPOSITION OF A INTO L AND U DOES NOT DEPEND ON B
C      A VECTOR Z FOR EACH X AND Y EQUATION WILL BE COMPUTED SUCH THAT
C      LZ=B,      Z FOR X IN COEF(I,3,1) AND FOR Y IN COEF(I,3,2)
C
C      COEF(1,3,1)=COEF(1,3,1)/COEF(1,1,1)
C      COEF(1,3,2)=COEF(1,3,2)/COEF(1,1,1)
C      COEF(1,1,2)=COEF(1,1,1)
DO 50 I=2,N
IM=I-NONE
COEF(1,2,2)=COEF(1,2,1)
COEF(IM,4,2)=COEF(IM,4,1)/COEF(IM,1,2)
COEF(I,1,2)=COEF(I,1,1)-COEF(IM,4,2)*COEF(I,2,2)
COEF(I,3,1)=(COEF(I,3,1)-COEF(I,2,2)*COEF(IM,3,1))/COEF(I,1,2)
COEF(I,3,2)=(COEF(I,3,2)-COEF(I,2,2)*COEF(IM,3,2))/COEF(I,1,2)
50 CONTINUE
C
C      COMPUTE VECTOR R BY BACK SUBSTITUTION WHERE UR=Z   R IN COEF(I,3,1)
C      FOR X AND IN COEF(I,3,2) FOR Y      THE R VECTOR IS THE FINAL
C      SOLUTION VECTOR FOR THE SLUPES
C
DO 60 I=1,N1
NN=N-I
COEF(NN,3,1)=COEF(NN,3,1)-COEF(NN,4,2)*COEF(NN+1,3,1)
COEF(NN,3,2)=COEF(NN,3,2)-COEF(NN,4,2)*COEF(NN+1,3,2)
60 CONTINUE
C
C      COMPUTE CUBIC COEFFICIENTS   FOR I-TH SEGMENT- X EQ. IS
C      X(T)=COEF(I,1,1)*T**3+COEF(I,2,1)*T**2+COEF(I,3,1)*T+COEF(I,4,1)
C
DO 70 I=1,N1
EL1=JNE/ELEN(I)
EL2=EL1*EL1
EL3=EL2*EL1
IP=I+NONE
X1=PNT(I,1)-PNT(IP,1)
Y1=PNT(I,2)-PNT(IP,2)
COEF(I,1,1)=TWO*EL3*X1+EL2*(COEF(I,3,1)+COEF(IP,3,1))
COEF(I,1,2)=TWO*EL3*Y1+EL2*(COEF(I,3,2)+COEF(IP,3,2))
COEF(I,2,1)=THREE*EL2*(-X1)-EL1*(TWO*COEF(I,3,1)+COEF(IP,3,1))
COEF(I,2,2)=THREE*EL2*(-Y1)-EL1*(TWO*COEF(I,3,2)+COEF(IP,3,2))
COEF(I,4,1)=PNT(I,1)
COEF(I,4,2)=PNT(I,2)
70 CONTINUE
RETURN
END

```

APPENDIX A - Continued

Subroutine CVRTV

```

SUBROUTINE CVRTV(NPTIN,NPORT,JVGS,IDIVC,IVGS)
DIMENSION JVGS(1),IVGS(1),IDIVC(1)
NSEG=NPTIN-1
ISUM=1
DO 8 I=1,NSEG
DO 6 J=1,NPORT
JVG=JVGS(J)
IF(JVG.EQ.1) GO TO 4
GO TO 6
4 IVGS(J)=ISUM
J=NPORT
6 CONTINUE
ISUM=ISUM+IDIVC(I)
8 CONTINUE
RETURN
END

```

Subroutine CROUT1

```

C SUBROUTINE CROUT1(C,S,N,IUM,ISYM,IWR)
C SET ISYM = 0 IF MATRIX IS SYMMETRIC
C SET IWR=0 OR NEGATIVE TO AVOID WRITEOUT
COMPLEX C(IUM,IUM),S(IUM)
COMPLEX SS
COMPLEX F,G,H,P,T,U
2 FORMAT(1X,1I10,1F15.3,1F15.0,2E15.4)
5 FORMAT(1HO)
IF(N.EQ.1)S(1)=S(1)/C(1,1)
IF(N.EQ.1)GO TO 100
IF(ISYM.NE.0)GO TO 8
DO 6 I=1,N
DO 6 J=I,N
C(J,I)=C(I,J)
6 CONTINUE
8 CONTINUE
F=C(1,1)
DO 10 L=2,N
G=C(1,L)
10 C(1,L)=G/F
DO 20 L=2,N
LLL=L-1
DO 20 I=L,N
F=C(I,L)
DO 11 K=1,LLL
G=C(I,K)
H=C(K,L)
11 F=F-G*H
C(I,L)=F
IF(L.EQ.1)GO TO 20
P=C(L,L)
IF(ISYM.EQ.0)GO TO 15
F=C(L,I)
DO 12 K=1,LLL
G=C(L,K)
H=C(K,I)
12

```

APPENDIX A - Continued

```

12   F=F-G*M
    C(L,I)=F/P
    GO TO 20
15   F=C(I,L)
    C(L,I)=F/P
20   CONTINUE
    DO 30 L=1,N
    P=C(L,L)
    T=S(L)
    IF(L.EQ.1) GO TO 20
    LLL=L-1
    DO 25 K=1,LLL
    F=C(L,K)
    U=S(K)
25   T=T-F*U
30   S(L)=T/P
    DO 35 L=2,N
    I=N-L+1
    II=I+1
    T=S(II)
    DO 35 K=II,N
    F=C(I,K)
    U=S(K)
35   T=T-F*U
38   S(I)=T
    IF(IWR.LE.0) GO TO 50
    CNDR=.0
    DO 40 I=1,N
    SS=S(I)
    SA=CABS(SS)
    IF(SA.GT.CNDR)CNDR=SA
40   CONTINUE
    DO 44 I=1,N
    SS=S(I)
    SA=CABS(SS)
    SNDR=.0
    IF(CNDR.GT.0.)SNDR=SA/CNDR
    SR=REAL(SS)
    SI=AIMAG(SS)
    PH=.0
    IF(SA.GT.0.)PH=57.29578*ATAN2(SI,SR)
    WRITE(6,2)I,SNDR,PH,SR,SI
44   CONTINUE
    WRITE(6,5)
50   CONTINUE
100  RETURN
    END

```

Subroutine CROUT2

```

C   SUBROUTINE CROUT2(C,S,N,IUM,ISYM,IWR)
C   SET ISYM = 0 IF MATRIX IS SYMMETRIC
C   SET IWR=0 OR NEGATIVE TO AVOID WRITEOUT
COMPLEX C(IUM,IUM),S(IUM)
COMPLEX SS
COMPLEX F,G,H,P,T,U
2   FORMAT(1X,1110,1H19.2,1H15.0,2E15.4)

```

APPENDIX A – Continued

```

5   FORMAT(1H0)
DC 30 L=1,N
P=C(L,L)
T=S(L)
IF(L.EQ.1)GO TO 30
LLL=L-1
DO 25 K=1,LLL
F=C(L,K)
U=S(K)
25 T=T-F*U
30 S(L)=T/P
DO 38 L=2,N
I=N-L+1
II=I+1
T=S(II)
DO 35 K=II,N
F=C(I,K)
U=S(K)
35 T=T-F*U
38 S(I)=T
IF(IWR.LE.0) GO TO 50
CNDR=.0
D.J 40 I=1,N
SS=S(I)
SA=CABS(SS)
IF(SA.GT.CNDR)CNCR=SA
40 CONTINUE
D.J 44 I=1,N
SS=S(I)
SA=CABS(SS)
SNJR=.0
IF(CNDR.GT.J,.1)SNOR=SA/CNDR
SR=REAL(SS)
SI=AIMAG(SS)
PH=.0
IF(SA.GT.0.)PH=57.29578*ATAN2(SI,SR)
WRITE(6,2)I,SNCR,PH,SR,SI
44 CONTINUE
WRITE(6,5)
50 CONTINUE
100 CONTINUE
RETURN
END

```

Subroutine SMM1

```

SUBROUTINE SMM1(UK,ZM11,ZM12)
COMPLEX ZM11,ZM12
COMPLEX H0,H1
DATA PI/3.14159/
CDK=COS(UK)
SDK=SIN(UK)
CALL HANK(UK,H0,H1)
SDKS=SDK**2
CDKS=CDK**2
ZM11=2.*H1*CDK-HC*SDK-2.*(.0,1.)*(1.+CDKS)/PI/UK
ZM12=HC*CDK*SDK-H1*(1.+CDKS)+4.*(.0,1.)*CDK/PI/UK
ZM11=15.*UK*ZM11/SDKS
ZM12=15.*UK*ZM12/SDKS
RETURN
END

```

APPENDIX A - Continued

Subroutine SMM2

```

SUBROUTINE SMM2(X1,Y1,X2,Y2,X3,Y3,DK1,DK2,INT,S11,S12,S21,S22)
COMPLEX SX1,Sx2
COMPLEX S11,S12,S21,S22
COMPLEX G11,G12,G21,G22
COMPLEX HC,H1,FFC,HH1
COMPLEX F(3)
COMPLEX AA(11,5),BA(11,5),CA(11,3),ZA(11,13)
COMPLEX AB(11,5),BB(11,5),CB(11,3),ZB(11,13)
COMPLEX AC(11,5),BC(11,5),CC(11,3),ZC(11,13)
COMPLEX AD(11,5),BD(11,5),CD(11,3),ZD(11,13)
EQUIVALENCE (ZA(1,1),AA(1,1)),(ZA(1,5),BA(1,1)),(ZA(1,11),CA(1,1))
EQUIVALENCE (ZB(1,1),AB(1,1)),(ZB(1,5),BB(1,1)),(ZB(1,11),CB(1,1))
EQUIVALENCE (ZC(1,1),AC(1,1)),(ZC(1,5),BC(1,1)),(ZC(1,11),CC(1,1))
EQUIVALENCE (ZD(1,1),AD(1,1)),(ZD(1,5),BD(1,1)),(ZD(1,11),CD(1,1))
DATA P1/3.14159/
DATA G,H/.314159,.261799/
DATA AA/
( 0.0 , 0.0 , 0.0 , 0.0 , 0.0 ),( 0.0 , 0.0 , 0.0 , 0.0 , 0.0 ),
( 0.0 , 0.0 , 0.0 , 0.0 , 0.0 ),( 0.0 , 0.0 , 0.0 , 0.0 , 0.0 ),
( 0.0 , 0.0 , 0.0 , 0.0 , 0.0 ),( 0.0 , 0.0 , 0.0 , 0.0 , 0.0 ),
(-0.000157,-0.005209),(-0.001205,-0.010471),(-0.003416,-0.014947),
(-0.006387,-0.017790),(-0.009493,-0.018725),(-0.011502,-0.018116),
(-0.012932,-0.016578),(-0.013971,-0.014465),(-0.015021,-0.011636),
(-0.01c041,-0.007672),(-0.0 , 0.0 ),(-0.004525,-0.020200),
(-0.004508,-0.040586),(-0.012827,-0.057989),(-0.024041,-0.069192),
(-0.035087,-0.073050),(-0.043494,-0.070898),(-0.048825,-0.065075),
(-0.052534,-0.057103),(-0.056248,-0.046623),(-0.060114,-0.032123),
( 0.0 , 0.0 ),(-0.001251,-0.042121),(-0.009051,-0.086548),
(-0.025857,-0.0122838),(-0.048756,-0.148317),(-0.071481,-0.157381),
(-0.088823,-0.153436),(-0.099479,-0.141631),(-0.106159,-0.125014),
(-0.112630,-0.104181),(-0.120115,-0.076060),(-0.0 , 0.0 ),
(-0.001879,-0.071060),(-0.013644,-0.142381),(-0.039218,-0.204035),
(-0.074406,-0.245482),(-0.109840,-0.262081),(-0.136913,-0.256958),
(-0.152731,-0.237878),(-0.160875,-0.211618),(-0.167710,-0.179818),
(-0.178957,-0.135049)/
DATA BA/
( 0.0 , 0.0 ),(-0.002341,-0.100292),(-0.017072,-0.200445),
(-0.049401,-0.287561),(-0.094491,-0.347606),(-0.140551,-0.373563),
(-0.175815,-0.368409),(-0.19020,-0.342136),(-0.201470,-0.305169),
(-0.203665,-0.262476),(-0.208911,-0.212054),(-0.0 , 0.0 ),
(-0.002513,-0.126603),(-0.018412,-0.252138),(-0.053664,-0.361786),
(-0.103547,-0.439113),(-0.155290,-0.474822),(-0.194970,-0.470681),
(-0.214671,-0.437498),(-0.215903,-0.388772),(-0.207611,-0.333925),
(-0.200231,-0.274917),(-0.0 , 0.0 ),(-0.002348,-0.145669),
(-0.017286,-0.288743),(-0.050747,-0.413776),(-0.098784,-0.503510),
(-0.149377,-0.547042),(-0.186217,-0.544154),(-0.205396,-0.504588),
(-0.199602,-0.443077),(-0.177390,-0.372977),(-0.151496,-0.301724),
( 0.0 , 0.0 ),(-0.018976,-0.153463),(-0.013976,-0.302360),
(-0.041308,-0.431868),(-0.081075,-0.525634),(-0.123553,-0.572360),
(-0.156179,-0.569787),(-0.168778,-0.525037),(-0.157527,-0.451540),
(-0.126031,-0.364194),(-0.085294,-0.274971),(-0.0 , 0.0 ),
(-0.001252,-0.146683),(-0.009304,-0.285862),(-0.027837,-0.407392),
(-0.053025,-0.494363),(-0.084419,-0.537583),(-0.106997,-0.533585),
(-0.114523,-0.486425),(-0.102426,-0.406260),(-0.071196,-0.306432),
(-0.025934,-0.200279)/
DATA CA/
( 0.0 , 0.0 ),(-0.000631,-0.123193),(-0.004700,-0.238814),
(-0.014034,-0.336302),(-0.027853,-0.405296),(-0.043016,-0.438105),
(-0.054629,-0.431450),(-0.057994,-0.387153),(-0.049893,-0.311671),

```

APPENDIX A – Continued

```

•(-0.029555,-0.214744),(-0.001190,-0.107643),(-0.0      , 0.0      ),  

•(-0.000169,-0.082703),(-0.001262,-0.158761),(-0.003760,-0.221141),  

•(-0.007539,-0.263649),(-0.011564,-0.281895),(-0.014831,-0.273976),  

•(-0.015658,-0.240766),(-0.013104,-0.185809),(-0.006753,-0.114839),  

•(-0.003082,-0.035048),(-0.0      , 0.0      ),(-0.0      , 0.0      ),  

•( 0.0      , 0.0      ),(-0.0      , 0.0      ),(-0.0      , 0.0      ),  

•( 0.0      , 0.0      ),(-0.0      , 0.0      ),(-0.0      , 0.0      ),  

•( 0.0      , 0.0      ),(-0.0      , 0.0      ),(-0.0      , 0.0      ),  

DATA AB/  

•( 0.0      , 0.0      ),(-0.0      , 0.0      ),(-0.0      , 0.0      ),  

•( 0.0      , 0.0      ),(-0.0      , 0.0      ),(-0.0      , 0.0      ),  

•( 0.0      , 0.0      ),(-0.0      , 0.0      ),(-0.0      , 0.0      ),  

•( 0.0      , 0.0      ),(-0.0      , 0.0      ),(-0.0      , 0.0      ),  

•(-0.003340,-0.004419),(-0.002298,-0.090521),(-0.006166,-0.012438),  

•(-0.010691,-0.013477),(-0.014254,-0.012457),(-0.016104,-0.010646),  

•(-0.016618,-0.009173),(-0.016583,-0.008348),(-0.015410,-0.007906),  

•(-0.016041,-0.007672),(-0.0      , 0.0      ),(-0.001233,-0.017091),  

•(-0.008606,-0.035027),(-0.023189,-0.048331),(-0.040403,-0.052781),  

•(-0.054100,-0.049271),(-0.061234,-0.042525),(-0.063056,-0.035971),  

•(-0.062600,-0.034006),(-0.061551,-0.032676),(-0.060114,-0.032123),  

•( 0.0      , 0.0      ),(-0.002470,-0.036321),(-0.017311,-0.074457),  

•(-0.046949,-0.103416),(-0.082436,-0.114318),(-0.111144,-0.108359),  

•(-0.126161,-0.054901),(-0.129404,-0.083489),(-0.127208,-0.077792),  

•(-0.123999,-0.076101),(-0.120115,-0.075060),(-0.0      , 0.0      ),  

•(-0.003713,-0.059481),(-0.026160,-0.121893),(-0.071555,-0.170647),  

•(-0.126915,-0.191508),(-0.172655,-0.184997),(-0.198694,-0.164838),  

•(-0.200504,-0.146686),(-0.193918,-0.138021),(-0.185403,-0.137040),  

•(-0.176967,-0.139049)/  

DATA BB/  

•( 0.0      , 0.0      ),(-0.004629,-0.083280),(-0.032827,-0.170404),  

•(-0.090683,-0.240484),(-0.162744,-0.274343),(-0.223733,-0.270515),  

•(-0.255911,-0.245296),(-0.258573,-0.220C35),(-0.243987,-0.207405),  

•(-0.225543,-0.207119),(-0.208911,-0.212C54),(-0.0      , 0.0      ),  

•(-0.004975,-0.104115),(-0.055111,-0.212304),(-0.099148,-0.301627),  

•(-0.180198,-0.349537),(-0.250040,-0.351579),(-0.287750,-0.323805),  

•(-0.287394,-0.291119),(-0.261916,-0.271716),(-0.229114,-0.268977),  

•(-0.200230,-0.274917),(-0.0      , 0.0      ),(-0.004651,-0.118450),  

•(-0.055441,-0.240050),(-0.094300,-0.342317),(-0.173687,-0.401796),  

•(-0.244239,-0.411004),(-0.201595,-0.382965),(-0.277350,-0.342543),  

•(-0.241536,-0.312267),(-0.193866,-0.300520),(-0.151496,-0.301724),  

•( 0.0      , 0.0      ),(-0.003747,-0.122174),(-0.027115,-0.247208),  

•(-0.077274,-0.352148),(-0.142916,-0.416420),(-0.204527,-0.430762),  

•(-0.236603,-0.403660),(-0.229491,-0.356579),(-0.189144,-0.512600),  

•(-0.133703,-0.285447),(-0.083294,-0.274971),(-0.0      , 0.0      ),  

•(-0.002503,-0.1158t1),(-0.018211,-0.229262),(-0.052342,-0.324015),  

•(-0.098474,-0.382853),(-0.141226,-0.397007),(-0.163819,-0.370954),  

•(-0.156510,-0.320632),(-0.121514,-0.266362),(-0.072004,-0.224233),  

•(-0.022934,-0.200279)/  

DATA CB/  

•( 0.0      , 0.0      ),(-0.031253,-0.094807),(-0.009157,-0.183962),  

•(-0.026492,-0.255549),(-0.050200,-0.298099),(-0.072543,-0.305734),  

•(-0.084314,-0.281122),(-0.079517,-0.234818),(-0.058378,-0.181876),  

•(-0.027802,-0.126541),(-0.001190,-0.107643),(-0.0      , 0.0      ),  

•(-0.000336,-0.058491),(-0.032462,-0.110535),(-0.007153,-0.148965),  

•(-0.013629,-0.168440),(-0.019770,-0.167176),(-0.023005,-0.147751),  

•(-0.021507,-0.11c582),(-0.015100,-0.082239),(-0.005851,-0.053094),  

•( 0.003082,-0.025047),(-0.0      , 0.0      ),(-0.0      , 0.0      ),  

•( 0.0      , 0.0      ),(-0.0      , 0.0      ),(-0.0      , 0.0      ),  

•( 0.0      , 0.0      ),(-0.0      , 0.0      ),(-0.0      , 0.0      ),  


```

APPENDIX A – Continued

DATA AC/

```

•( 0.0      , 0.0      ),( 0.0      , 0.0      ),( 0.0      , 0.0      ),
•( 0.0      , 0.0      ),( 0.0      , 0.0      ),( 0.0      , 0.0      ),
•( 0.0      , 0.0      ),( 0.0      , 0.0      ),( 0.0      , 0.0      ),
•( 0.0      , 0.0      ),( 0.0      , 0.0      ),( 0.0      , 0.0      ),
•( 0.000157, 0.005082), ( 0.001201, 0.009480), ( 0.003357, 0.011733),
•( 0.005987, 0.010617), ( 0.007728, 0.005929), ( 0.007122,-0.001153),
•( 0.003386,-0.008306), (-0.003018,-0.012842), (-0.010334,-0.012768),
•(-0.016041,-0.007672), ( 0.0      , 0.0      ), ( 0.000625, 0.019708),
•( 0.004494, 0.036757), ( 0.012606, 0.045606), ( 0.022612, 0.041617),
•( 0.029476, 0.023948), ( 0.027707,-0.003090), ( 0.014203,-0.030841),
•(-0.009630,-0.049148), (-0.037502,-0.050247), (-0.060114,-0.032123),
•( 0.0      , 0.0      ), ( 0.001251, 0.042077), ( 0.009025, 0.078434),
•( 0.025459, 0.097687), ( 0.046091, 0.090218), ( 0.061025, 0.054388),
•( 0.059152,-0.001720), ( 0.033682,-0.063742), (-0.013504,-0.101986),
•(-0.070820,-0.108932), (-0.120115,-0.076060), ( 0.0      , 0.0      ),
•( 0.001878, 0.069353), ( 0.013509, 0.029150), ( 0.038676, 0.161592),
•( 0.070870, 0.151890), ( 0.045735, 0.096691), ( 0.056450, 0.008192),
•( 0.061778,-0.087762), (-0.007330,-0.155430), (-0.095565,-0.180229),
•(-0.176966,-0.139049)

```

DATA BC/

```

•( 0.0      , 0.0      ), ( 0.002340, 0.097909), ( 0.017036, 0.182031),
•( 0.048831, 0.228837), ( 0.096759, 0.219080), ( 0.125444, 0.148077),
•( 0.131951, 0.030721), ( 0.094532,-0.100692), ( 0.012912,-0.205636),
•(-0.098307,-0.248638), (-0.208911,-0.212054), ( 0.0      , 0.0      ),
•( 0.002512, 0.123636), ( 0.01e381, 0.0229304), ( 0.053174, 0.289463),
•( 0.100303, 0.282269), ( 0.042107, 0.020389), ( 0.156246, 0.066072),
•( 0.125019,-0.091267), ( 0.043959,-0.224663), (-0.073914,-0.293479),
•(-0.200230,-0.274917), ( 0.0      , 0.0      ), ( 0.002348, 0.142316),
•( 0.017264, 0.253045), ( 0.05e406, 0.0332991), ( 0.096514, 0.330174),
•( 0.140090, 0.249802), ( 0.0160697, 0.0108489), ( 0.140980,-0.058585),
•( 0.074360,-0.207009), (-0.050665,-0.296164), (-0.151456,-0.301725),
•( 0.0      , 0.0      ), ( 0.001890, 0.150007), ( 0.013964, 0.275992),
•( 0.041123, 0.349639), ( 0.075e41, 0.351277), ( 0.118501, 0.277962),
•( 0.141190, 0.146142), ( 0.033630,-0.011777), ( 0.089045,-0.156080),
•( 0.011706,-0.25C991), (-0.083294,-0.274971), ( 0.0      , 0.0      ),
•( 0.031252, 0.143458), ( 0.005359, 0.0262368), ( 0.027766, 0.331649),
•( 0.054554, 0.335798), ( 0.082517, 0.0274561), ( 0.101461, 0.163812),
•( 0.101866, 0.031562), ( 0.078589,-0.089743), ( 0.033201,-0.172247),
•(-0.025934,-0.200279)

```

DATA CC/

```

•( 0.0      , 0.0      ), ( 0.000631, 0.120521), ( 0.004699, 0.218624),
•( 0.014019, 0.274433), ( 0.027797, 0.277569), ( 0.042655, 0.230437),
•( 0.053695, 0.147572), ( 0.056225, 0.051447), ( 0.047541,-0.033974),
•( 0.027976,-0.065911), ( 0.001190,-0.107643), ( 0.0      , 0.0      ),
•( 0.000169, 0.080793), ( 0.001262, 0.144415), ( 0.003779, 0.177640),
•( 0.007537, 0.175275), ( 0.011670, 0.141517), ( 0.014905, 0.088406),
•( 0.016006, 0.031965), ( 0.014228,-0.012695), ( 0.009626,-0.035735),
•( 0.003082,-0.035048), ( 0.0      , 0.0      ), ( 0.0      , 0.0      ),
•( 0.0      , 0.0      ), ( 0.0      , 0.0      ), ( 0.0      , 0.0      ),
•( 0.0      , 0.0      ), ( 0.0      , 0.0      ), ( 0.0      , 0.0      )

```

DATA AD/

```

•( 0.0      , 0.0      ), ( 0.0      , 0.0      ), ( 0.0      , 0.0      ),
•( 0.0      , 0.0      ), ( 0.0      , 0.0      ), ( 0.0      , 0.0      ),
•( 0.0      , 0.0      ), ( 0.0      , 0.0      ), ( 0.0      , 0.0      ),
•( 0.0      , 0.0      ), ( 0.0      , 0.0      ), ( 0.0      , 0.0      ),
•( 0.000350, 0.004351), ( 0.004288, 0.008488), ( 0.006025, 0.010438),
•( 0.009831, 0.008609), ( 0.011267, 0.004234), ( 0.008556,-0.003540),
•( 0.002400,-0.008933), (-0.005336,-0.011221), (-0.011981,-0.010192),

```

APPENDIX A - Continued

```

•(-0.016041,-0.007672),(.0.0      , 0.0      ),( 0.001233, 0.016831),
•( 0.008573, 0.032883),(.0.022693, 0.040770),(.0.037426, 0.034397),
•( 0.043448, 0.014346),(.0.034458,-0.011650),( 0.011460,-0.033113),
•(-0.017799,-0.042916),(-0.043658,-0.040804),(-0.060114,-0.032123),
•(.0.0      , 0.0      ),(.0.002470, 0.035786),(.0.017250, 0.070056),
•( 0.046051, 0.067972),(.0.077002, 0.076856),(.0.091497, 0.036918),
•( 0.076138,-0.017229),(.0.031538,-0.064626),(-0.027930,-0.089832),
•(-0.082918,-0.090514),(-0.120115,-0.075050),(.0.0      , 0.0      ),
•( 0.003712, 0.056644),(.0.026082, 0.0115048),(.0.070396, 0.146811),
•( 0.119825, 0.133934),(.0.146662, 0.074822),(.0.129375,-0.010454),
•( 0.066115,-0.090716),(-0.024054,-0.140662),(-0.112498,-0.153109),
•(-0.176986,-0.139049)//
      DATA BU/
•( 0.0      , 0.0      ),(.0.004628, 0.082184),(.0.032749, 0.161505),
•( 0.089520, 0.205979),(.0.155540, 0.200706),(.0.195878, 0.1293d1),
•( 0.184909, 0.017794),(.0.115300,-0.096151),(.0.001649,-0.178288),
•(-0.115838,-0.214174),(-0.208911,-0.212054),(.0.0      , 0.0      ),
•( 0.004974, 0.102873),(.0.035451, 0.202291),(.0.098233, 0.267494),
•( 0.174443, 0.2e8419),(.0.228664, 0.196367),(.0.228486, 0.071031),
•( 0.162555,-0.068660),(.0.04e529,-0.183608),(-0.085834,-0.251922),
•(-0.200230,-0.274917),(.0.0      , 0.0      ),(.0.004650, 0.117229),
•( 0.033406, 0.230289),(.0.043850, 0.309461),(.0.170260, 0.324651),
•( 0.250890, 0.264202),(.0.244309, 0.142450),(.0.195843,-0.006541),
•( 0.094614,-0.144625),(-0.031874,-0.245375),(-0.151496,-0.301724),
•( 0.0.0      , 0.0      ),(.0.005747, 0.122169),(.0.027103, 0.239244),
•( 0.077090, 0.325669),(.0.142097, 0.358050),(.0.199560, 0.314887),
•( 0.221934, 0.213275),(.0.193194, 0.075462),(.0.122273,-0.066987),
•( 0.021307,-0.188174),(-0.083294,-0.274971),(.0.0      , 0.0      ),
•( 0.002503, 0.115253),(.0.018213, 0.224467),(.0.052364, 0.308184),
•( 0.090584, 0.346406),(.0.141473, 0.328253),(.0.1e3807, 0.256767),
•( 0.154392, 0.147472),(.0.112575, 0.022151),(.0.047622,-0.098570),
•(-0.025933,-0.200279)//
      DATA CD/
•( 0.0      , 0.0      ),(.0.001253, 0.094692),(.0.009162, 0.183015),
•( 0.026560, 0.252210),(.0.050653, 0.289695),(.0.074115, 0.287980),
•( 0.088393, 0.247268),(.0.087403, 0.175067),(.0.069807, 0.083426),
•( 0.038988,-0.014601),(.0.001190,-0.107643),(.0.0      , 0.0      ),
•( 0.000336, 0.058756),(.0.002464, 0.112516),(.0.007181, 0.154899),
•( 0.013806, 0.180161),(.0.020446, 0.184720),(.0.024829, 0.168007),
•( 0.025253, 0.132455),(.0.021189, 0.082759),(.0.013315, 0.024850),
•( 0.003082,-0.035047),(.0.0.0      , 0.0      ),(.0.0      , 0.0      ),
•( 0.0      , 0.0      ),(.0.0      , 0.0      ),(.0.0      , 0.0      ),
•( 0.0      , 0.0      ),(.0.0      , 0.0      ),(.0.0      , 0.0      )//
DKM=DK1
IF(DK2.GT.DK1)DKM=DK2
IF(DKM.LT.3.)GO TO 42
CALL ZMM2(X1,Y1,X2,Y2,X3,Y3,DK1,DK2,INT,S11,S12,S21,S22)
RETURN
10 CONTINUE
DK=(DK1+DK2)/2.
PD=100.*ABS(DK2-DK1)/DK
IF(PD.LT.3.)GO TO 42
CALL ZMM2(X1,Y1,X2,Y2,X3,Y3,DK1,DK2,INT,S11,S12,S21,S22)
RETURN
42 CONTINUE
DKS=DK1*DK2

```

APPENDIX A – Continued

```

CDK=CDK(DK)
SDK=SIN(DK)
SDKS=SDK**2
CDKS=CDK**2
CBET=(X2-X1)/DK1
SBET=(Y2-Y1)/DK1
XB=(X3-X1)*CBET+(Y3-Y1)*SBET
YB=-(X3-X1)*SBET+(Y3-Y1)*CBET
CAL=(AB-DK1)/DK2
SAL=ABS(YB)/DK2
CALL HANK(DK,H0,H1)
IF(CAL.LT.0.)GO TO 50
IF(SAL.GT..04)GO TO 50
CNT=15.*DK*CAL/SDKS
CALL HANK(2.*DK,H0,HH1)
S11=CNT*(2.*HH1*CDK-H0*SDK*CDK-H1*(1.+CDKS)+2.*(.0,1.)*CDK/PI/DK)
S12=CNT*(2.*HH0*SDK*CDK-2.*HH1*CDKS
2+2.*H1*CDK-H0*SDK-2.*(.0,1.)/PI/DK)
S21=CNT*(2.*H1*CDK+H0*SLK-2.*HH1-2.*(.0,1.)*CDKS/PI/DK)
S22=CNT*(H0*CDK+SDK-H1*(1.+CDKS)-2.*HH0*SDK
2+2.*HH1*CDK+2.*(.0,1.)*CDK/PI/DK)
RETURN
50 CONTINUE
F(1)=H0
S11= DK*(-H1+2.*(.0,1.)*CDK/PI/DK)
S12=- DK*(SDK*H0-CDK*H1+2.*(.0,1.)/PI/DK)
S21= DK*(CDK*H1-2.*(.0,1.)*CDKS/PI/DK)
S22= DK*CDK*(SLK*H0-CDK*H1+2.*(.0,1.)/PI/DK)
AL=1.570796
IF(CAL.NE.0.)AL=ATAN2(SAL,CAL)
AL=ABS(AL)
IF(AL.GT.2.0)GO TO 82
TK=DK/2.
DO 80 J=2,3
TKS=TK**2
RK=SWKT(DKS+2.*DK*TK*CAL+TKS)
CALL HANK(RK,H0,F1)
F(J)=H0
TK=DK
80 CONTINUE
SA=1.+SDK/DK+4.*(CDK-1.)/DKS
SB=8.*(.1.-CDK)/DKS-4.*SDK/DK
SC=3.*SDK/DK-CDK+4.*(CDK-1.)/DKS
S11=S11+CDK*(SC*F(1)+SB*F(2)+SA*F(3))
S12=S12+CDK*(SA*F(1)+SB*F(2)+SC*F(3))
S21=S21-(SC*F(1))+SB*F(2)+SA*F(3))
S22=S22-(SA*F(1))+SB*F(2)+SC*F(3))
GO TO 98
82 CONTINUE
SA1=(.0,.0)
SA2=(.0,.0)
INP=2*(INT/2)
FIT=INP
IP=INP+1
DT=DK/FIT
TK=.0
SGI=-1.
DO 90 I=1,IP
D=SGI+3.
IF(.1.EQ.1)D=1.

```

APPENDIX A - Continued

```

IF(I.EQ.IP)D=1.
TKS=TK**2
RK=SQRT(DKS+2.*DK*TK*CAL+TKS)
CALL HANK(RK,HC,H1)
S1=SIN(DK-TK)
S2=SIN(TK)
SX1=SX1+S1*H0*D
SX2=SX2+S2*H0*D
SGI=-SGI
TK=TK+DT
90 CONTINUE
SX1=SX1*DT/3.
SX2=SX2*DT/3.
S11=S11+CDK*SX1
S12=S12+CDK*SX2
S21=S21-SX1
S22=S22-SX2
99 CONTINUE
X=DK/G
I=K+1.5
IF(I.LT.2)I=2
IF(I.GT.10)I=10
IM=I-1
IP=I+1
Y=AL/H
J=Y+1.5
IF(J.LT.2)J=2
IF(J.GT.12)J=12
JM=J-1
JP=J+1
FI=I
FJ=J
XF=FI-1.
YJ=FJ-1.
P=X-XI
Q=Y-YJ
PT=P/2.
WT=Q/2.
A=PT*(P-1.)
B=PT*(P+1.)
C=WT*(Q-1.)
D=WT*(Q+1.)
E=1.-P**2-Q**2
G11=A*ZA(IM,J)+B*ZA(IP,J)+C*ZA(I,JM)+D*ZA(I,JP)+E*ZA(I,J)
G12=A*ZB(IM,J)+B*ZB(IP,J)+C*ZB(I,JM)+D*ZB(I,JP)+E*ZB(I,J)
G21=A*ZC(IM,J)+B*ZC(IP,J)+C*ZC(I,JM)+D*ZC(I,JP)+E*ZC(I,J)
G22=A*ZD(IM,J)+B*ZD(IP,J)+C*ZD(I,JM)+D*ZD(I,JP)+E*ZD(I,J)
CCC=15./SIKS
S11=CCC*(CAL*S11+G11*DK)
S12=CCC*(CAL*S12+G12*DK)
S21=CCC*(CAL*S21+G21*DK)
S22=CCC*(CAL*S22+G22*DK)
RETURN
END

```

APPENDIX A – Continued

Subroutine ZMM2

```

SUBROUTINE ZMM2(X1,Y1,X2,Y2,X3,Y3,DK1,DK2,INT,S11,S12,S21,S22)
COMPLEX RKH1
COMPLEX Sx1,Sx2
COMPLEX S11,S12,S21,S22
COMPLEX Y11,Y12,Y21,Y22
COMPLEX EY1,EY2
COMPLEX HO,H1,HHC,HH1,SH0,SH1
COMPLEX DHH0,DHH1,DHC,DH1,DSH0,DSH1
COMPLEX DY11,DY12,DY21,DY22
COMPLEX CCP
COMPLEX FUN
COMPLEX F(3)
DATA CCP/(.0,.63E62)/
DKM=DK1
IF(DK2.GT.DK1)DKM=DK2
IF(DKM.LT.3.)GO TO 10
S11=(.0,.0)
S12=(.0,.0)
S21=(.0,.0)
S22=(.0,.0)
RETURN
10 CONTINUE
SUK1=SIN(DK1)
SUK2=SIN(DK2)
CDK1=COS(DK1)
CDK2=COS(DK2)
CBET=(X2-X1)/DK1
SBET=(Y2-Y1)/DK1
XB=(X3-X1)*CBET+(Y3-Y1)*SBET
YB=-(X3-X1)*SBET+(Y3-Y1)*CBET
CAL=(XB-DK1)/DK2
SAL=ABS(YB)/DK2
CALL HANK(DK2,HHC,HH1)
DHH0=DK2*HH0
DHH1=DK2*HH1
C1S2=CDK1*SUK2
C1C2=CDK1*CDK2
IF(CAL.LT.0.)GO TO 20
IF(SAL.GT..04)GO TO 20
CNT=15.*CAL/SUK1/SUK2
CALL HANK(DK1,HO,H1)
HO=DK1*HO
H1=DK1*H1
DKS=DK1+DK2
CALL HANK(DKS,SHC,SH1)
DSH0=DKS*SH0
LSH1=DKS*SH1
S11=INT*(CDK1*DSH1-C1S2*DHO-C1C2*DHC-CDK1*DHC+CCP*CDK2)
S12=INT*(CDK2*DHC-SUK2*DHH1-CDK1*SH0+C1S2*DSH0-C1C2*DSH1)
S21=INT*(SUK2*DHO-DSH1+CDK2*DHC+CDK1*DHC-CCP*C1C2)
S22=INT*(C1S2*DHO-C1C2*DSH1+CCP*CDK1*DHC-SUK2*DSH0+CDK2*DSH1)
RETURN
20 CONTINUE
S11=-DHH1+CCP*CDK2
S12=-SUK2*DHH0+CDK2*DHH1-CCP
S21=(DHH1-CCP*CDK2)*CDK1
S22=(SUK2*DHH0-CDK2*DHC+CCP)*CDK1
DKS1=DK1**2
AL=1.570796
IF(CAL.NE.0.)AL=ATAN2(SAL,CAL)

```

APPENDIX A - Continued

```

AL=ABS(AL)
INP=2*(INT/2)
FIT=INP
IP=INP+1
IF(AL.GT.2.0)GO TO 82
TK=.0
DO 80 J=1,3
TKS=TK**2
RK=SQRT(DKS1+2.*DK1*TK*CAL+TKS)
CALL HANK(RK,H0,H1)
F(J)=H0
TK=TK+DK2/2.
80 CONTINUE
DKS2=DK2**2
SA=1.+SLK2/DK2+4.*(CUK2-1.)/DKS2
SB=3.*((1.-CDK2)/DKS2-4.*SLK2/DK2
SC=3.*SLK2/DK2-CUK2+4.*((CUK2-1.)/DKS2
S11=S11+CDK1*(SC*F(1)+SB*F(2)+SA*F(3))
S12=S12+CDK1*(SA*F(1)+SB*F(2)+SC*F(3))
S21=S21-(SC*F(1)+SB*F(2)+SA*F(3))
S22=S22-(SA*F(1)+SB*F(2)+SC*F(3))
GU TO 98
82 CONTINUE
DT=DK2/FIT
TK=.0
SX1=(.0,.0)
SX2=(.0,.0)
SGI=-1.
DO 90 I=1,IP
D=SGI+3.
IF(I.EQ.1)D=1.
IF(I.EQ.IP)D=1.
TKS=TK**2
RK=SQRT(DKS1+2.*DK1*TK*CAL+TKS)
CALL HANK(RK,H0,H1)
S1=SIN(DK2-TK)
S2=SIN(TK)
SX1=SX1+S1*H0*D
SX2=SX2+S2*H0*D
SGI=-SGI
TK=TK+DT
90 CONTINUE
SX1=SX1*DT/3.
SX2=SX2*DT/3.
S21=S21-SX1
S22=S22-SX2
S12=S12+CDK1*SX2
S11=S11+CDK1*SX1
98 CONTINUE
JP=IP
Y11=(.0,.0)
Y12=(.0,.0)
Y21=(.0,.0)
Y22=(.0,.0)
B=.0
IF(AL.LT..05)GC TO 210
ALT=AL/2.
CALT=COS(ALT)
SALT=SIN(ALT)
RCP=(DK1+DK2)*CALT

```

APPENDIX A - Continued

```

RSP=(UK2-UK1)*SALT
PHC=ATAN2(RSP,RCP)
SGI=-1.
PH=-ALT
DPH=AL/FIT
DO 200 I=1,IP
D=SGI+3.
IF(I.EQ.1)D=1.
IF(I.EQ.IP)D=1.
SAP=SIN(ALT+PH)
SAM=SIN(ALT-PH)
IF(PH.LE.PHC)RMAX=DK1*SAL/SAM
IF(PH.GT.PHC)RMAX=DK2*SAL/SAM
URK=RMAX/FIT
RK=.0
SGJ=-1.
DY11=(.0,.0)
DY12=(.0,.0)
DY21=(.0,.0)
DY22=(.0,.0)
DO 100 J=1,JP
C=SGJ+3.
IF(J.EQ.1)C=1.
IF(J.EQ.JP)C=1.
CALL AHANK(RK,RKF1)
SK=RK*SAM/SAL
TK=RK*SAP/SAL
C1=CJS(SK)
C2=CJS(DK1-SK)
S1=SIN(DK2-TK)
S2=SIN(TK)
FUN=C*FRKH1
DY11=DY11-FUN*C1*S1
DY12=DY12-FUN*C1*S2
DY21=DY21+FUN*C2*S1
DY22=DY22+FUN*C2*S2
SGJ=-SGJ
RK=RK+URK
100 CONTINUE
B=SAP*URK*D
Y11=Y11+B*DY11
Y12=Y12+B*DY12
Y21=Y21+B*DY21
Y22=Y22+B*DY22
PH=PH+DPH
SGI=-SGI
200 CONTINUE
B=DPH/9.
210 CONTINUE
CNT=15./SDK1/SDK2
S11=cnt*(CAL*S11+B*Y11)
S12=cnt*(CAL*S12+B*Y12)
S21=cnt*(CAL*S21+B*Y21)
S22=cnt*(CAL*S22+B*Y22)
RETURN
END

```

APPENDIX A - Continued

Subroutine SMM3

```

SUBROUTINE SMM3(X1,Y1,X2,Y2,X3,Y3,X4,Y4,
2UK1,UK2,S11,S12,S21,S22)
COMPLEXA S11,S12,S21,S22
COMPLEX ET1,ET2
COMPLEX HO,H1
DIMENSION CC1(3C),SS1(3O),CC2(3O),SS2(3C)
S11=(.0,.0)
S12=(.0,.0)
S21=(.0,.0)
S22=(.0,.0)
C8LT=(X2-X1)/UK1
SBET=(Y2-Y1)/UK1
XA=(X3-X1)*CBET+(Y3-Y1)*SBET
XB=(X4-X1)*CBET+(Y4-Y1)*SBET
YA=-(X3-X1)*SBET+(Y3-Y1)*CBET
YB=-(X4-X1)*SBET+(Y4-Y1)*CBET
CAL=(XB-XA)/UK2
SAL=(YB-YA)/UK2
RMIN=10000.
X=XA
Y=YA
DO 40 J=1,2
YS=Y**2
XP=.0
DO 35 I=1,2
DX=X-XP
R=SQR(DX**2+YS)
IF(R.LT.RMIN)RMIN=R
XP=UK1
35 CONTINUE
A=XA+UK2*CAL
Y=YA+UK2*SAL
40 CONTINUE
ISS=4.*UK1/RMIN
ISS=2*(ISS/2)
IF(ISS.LT.2)ISS=2
IF(ISS.GT.10)ISS=10
FSS=ISS
ISW=ISS+1
US=UK1/FSS
ITT=4.*UK2/RMIN
ITT=2*(ITT/2)
IF(ITT.LT.2)ITT=2
IF(ITT.GT.10)ITT=10
FTT=ITT
ITQ=ITT+1
DT=UK2/FTT
XP=.0
SGN=-1.
DO 50 I=1,ISW
C=SGN+3.
IF(I.EQ.1)C=1.
IF(I.EQ.ISW)C=1.
CC1(I)=C*CCS(UK1-XP)
SS1(I)=C*SIN(UK1-XP)
CC2(I)=C*CUS(XP)
SS2(I)=C*SIN(XP)
SGN=-SGN
XP=XP+US
50 CONTINUE

```

APPENDIX A - Continued

```

DX=DT*CAL
DY=DT*SAL
X=XA
Y=YA
TK=.0
SGJ=-1.
DO 200 J=1,ITQ
D=SGJ+3.
IF(J.EQ.1)D=1.
IF(J.EQ.ITQ)D=1.
CT1=U*SIN(OK2-TK)
CT2=U*SIN(TK)
XP=.0
YS=Y**2
ET1=(.0,.0)
ET2=(.0,.0)
DO 100 I=1,ISQ
DELX=X-XP
RK=SQR(DELX**2+YS)
RDT=(DELX*CAL+Y*SAL)/RK
C1=CC1(I)
S1=SS1(I)
C2=CC2(I)
S2=SS2(I)
CALL HANK(RK,H0,H1)
ET1=ET1-(S1*H0*CAL+C1*H1*RDT)
ET2=ET2-(S2*H0*CAL-C2*H1*RDT)
XP=XP+U
100 CONTINUE
S11=S11+CT1*ET1
S12=S12+CT2*ET1
S21=S21+CT1*ET2
S22=S22+CT2*ET2
SGJ=-SGJ
TK=TK+UT
X=X+DX
Y=Y+DY
200 CONTINUE
CST=(15./9.)*DS*DT/SIN(OK1)/SIN(OK2)
S11=CST*S11
S12=CST*S12
S21=CST*S21
S22=CST*S22
RETURN
END

```

APPENDIX A - Continued

Subroutine HANK

```

SUBROUTINE HANK(X,H,H1)
COMPLEX H,H1
DATA TSP/.63662/
X=ABS(X)
IF(X.GT.3.)GO TO 100
XLN=ALUG(.5*X)
R1=X/3.
R2=R1*R1
R4=R2*R2
R6=R4*R2
IF(R1.GT..1)GO TO 50
D=-.516387*R6+1.26562*R4-2.*5*R2+1.
Y=.253301*R6-.743504*R4+.605594*R2+.367467
B1=X*(-.395429E-1*R6+.210936*R4+.5625*R2+.5)
Y1=(-1.31648*R6+2.16827*R4+.221209*R2-.63662)/X
Y=Y+TSP*XLN*B
Y1=Y1+TSP*XLN*B1
H=CMPLX(B,-Y)
H1=CMPLX(B1,-Y1)
RETURN
50 CONTINUE
R8=R4*R4
R10=R6*R4
R12=R6*R6
B=.21E-3*R12-.39444E-2*R10+.444479E-1*R8
2-.516387*R6+1.26562*R4-2.*5*R2+1.
Y=-.24846E-3*R12+.427315E-2*R10-.426121E-1*R8
2+.253301*R6-.743504*R4+.605594*R2+.367467
B1=X*(.1109E-4*R12-.31761E-3*R10+.443319E-2*R8
2-.395429E-1*R6+.210936*R4+.5625*R2+.5)
Y1=(.27873E-2*R12-.400976E-1*R10+.312395*R8
2-1.31648*R6+2.16827*R4+.221209*R2-.63662)/X
Y=Y+TSP*XLN*B
Y1=Y1+TSP*XLN*B1
H=CMPLX(B,-Y)
H1=CMPLX(B1,-Y1)
RETURN
100 CONTINUE
SW=SQRT(X)
R1=3./X
R2=R1*R1
R3=R1*R2
R4=R2*R2
R5=R3*R2
R6=R3*R3
F=.14476E-3*R6-.72805E-3*R5+.157237E-2*R4
2-.9512E-4*R3-.55274E-2*R2-.77E-6*R1+.757685
T=.15558E-3*R6-.29333E-3*R5-.54125E-3*R4
2+.262573E-2*R3-.3954L-4*R2-.41664E-1*R1-.785398*X
B=F*COS(T)/SW
Y=F*SIN(T)/SW
F=-.20039E-3*R6+.113653E-2*R5-.249511E-2*R4
2+.17105E-3*R3+.165967E-1*R2+.156E-5*R1+.757885
T=-.29166E-3*R6+.79824E-3*R5+.74348E-3*R4
2-.637879E-2*R3+.565E-4*R2+.124996*R1-2.35619*X
B1=F*COS(T)/SW
Y1=F*SIN(T)/SW
H=CMPLX(B,-Y)
H1=CMPLX(B1,-Y1)
RETURN
END

```

APPENDIX A - Continued

Subroutine XHANK

```

SUBROUTINE XHANK(X,XH)
COMPLEX XH
COMPLEX G(57)
DATA G/
  .( 0.0 , 0.636620),(.0.004994, 0.645895),( 0.019900, 0.664765),
  .( 0.044496, 0.687931),(.0.078411, 0.712349),( 0.121134, 0.735736),
  .( 0.172020, 0.756234),( 0.230297, 0.772274),( 0.295073, 0.782515),
  .( 0.365354, 0.785814),( 0.440050, 0.781213),( 0.517992, 0.767932),
  .( 0.597946, 0.745364),( 0.678530, 0.713076),( 0.758725, 0.670806),
  .( 0.836904, 0.618463),( 0.911833, 0.556125),( 0.982200, 0.484035),
  .( 1.046729, 0.402597),( 1.104198, 0.312372),( 1.153449, 0.214066),
  .( 1.193413, 0.108527),( 1.223118,-0.002272),( 1.241706,-0.120236),
  .( 1.248435,-0.241172),( 1.242755,-0.364794),( 1.224128,-0.489743),
  .( 1.192324,-0.614606),( 1.147186,-0.737925),( 1.088740,-0.858224),
  .( 1.017176,-0.974021),( 1.032857,-1.083849),( 0.836299,-1.186275),
  .( 0.728191,-1.279913),( 0.609559,-1.363450),( 0.480824,-1.435658),
  .( 0.34678,-1.495409),( 0.196189,-1.541694),( 0.048722,-1.573635),
  .(-0.106448,-1.590497),(-0.2c4170,-1.591702),(-0.423418,-1.576836),
  .(-0.582314,-1.545654),(-0.739152,-1.498094),(-0.892209,-1.434272),
  .(-1.039768,-1.354489),(-1.180140,-1.259230),(-1.311676,-1.149158),
  .(-1.432796,-1.025115),(-1.542001,-0.888112),(-1.637894,-0.739318),
  .(-1.719193,-0.380060),(-1.784758,-0.411793),(-1.833591,-0.236107),
  .(-1.864861,-0.054691),(-1.877910, 0.130665),(-1.872264, 0.318107)/
X=AUS(X)
IF(X.GT.5.6)GO TO 100
Y=1D.*X
J=Y+1.5
IF(J.LT.2)J=2
IF(J.GT.56)J=56
JM=J-1
JP=J+1
FJ=J
YJ=FJ-1.
Q=Y-YJ
QT=Q/2.
C=QT*(W-1.)
U=QT*(W+1.)
E=1.-Q**2
XH=C*G(JM)+D*G(JP)+E*G(J)
RETURN
100 CONTINUE
SW=SQRT(X)
R1=3./X
R2=R1*R1
R3=R1*R2
R4=R2*R2
R5=R3*R2
R6=R3*R3
F=-.20035E-3*R6+.113653E-2*R5-.249E11E-2*R4
2+.17105E-3*R3+.165957E-1*k2+.156E-5*R1+.797885
T=-.29166E-3*R6+.79824E-3*R5+.74348E-3*R4
Z-.657879E-2*R3+.565E-4*R2+.124995*R1-2.25619*X
B1=F*COS(T)*SW
Y1=F*SIN(T)*SW
XH=CMPLX(B1,-Y1)
RETURN
END

```

APPENDIX A - Continued

Subroutine CFF

```
SUBROUTINE CFF(XA,YA,XB,YB,DK,CPH,SPH,EP1,EP2)
COMPLEX EJA,EJB,EP1,EP2,SQJ,CST
SQJ=30.*(1.,1.)/1.414214
XAB=XB-XA
YAB=YB-YA
CA=XAB/DK
CB=YAB/DK
G=CA*CPH+CB*SPH
P=CB*CPH-CA*SPH
GK=P**2
EP1=(.0,.0)
EP2=(.0,.0)
IF(GK.LT..001) GO TO 200
A=XA*CPH+YA*SPH
B=XB*CPH+YB*SPH
EJA=CMPLX(COS(A),SIN(A))
EJB=CMPLX(COS(B),SIN(B))
SDK=SIN(DK)
CDK=COS(DK)
SGD=SIN(G*DK)
CGD=COS(G*DK)
CST=SQJ/(P*SDK)
EP1=CST*EJA*CMPLX(CDK-CGD,G*SDK-SGD)
EP2=CST*EJB*CMPLX(CDK-CGD,SGD-G*SDK)
200 CONTINUE
RETURN
END
```

APPENDIX A – Continued

Subroutine SKETCH

```

SUBROUTINE SKETCH(XCCOR,YCCCR,NPLOT,HPAT,NSKIPS,NSYMB,NSIZES,
1 IUNITS)
COMMON /BLK1/ KNTPLT,XNEW,YNEW
DIMENSION XCOR(1),YCOR(1)
KNTPLT=KNTPLT+1
WRITE(6,305) KNTPLT
IF(KNTPLT.EQ.1) GO TO 3
CALL CALPLT(XNEW,YNEW,-3)
3 CONTINUE
XMAX=0.
YMAX=0.
DO 4 I=1,NPLCT
XTST=XCOR(I)
XATST=ABS(XTST)
IF(XATST.GE.XTST) XMAX=XATST
YTST=YCOR(I)
YATST=ABS(YTST)
IF(YATST.GE.YMAX) YMAX=YATST
4 CONTINUE
ZMAX=XMAX
IF(YMAX.GE.XMAX) ZMAX=YMAX
SCALE=ZMAX/(C.2*HPAT)
HALF=0.2*HPAT
CALL CALPLT(-HALF,-HALF,3)
CALL CALPLT(HALF,-HALF,2)
CALL CALPLT(HALF,HALF,2)
CALL CALPLT(-HALF,HALF,2)
CALL CALPLT(-HALF,-HALF,2)
CALL CALPLT(-HALF,C.,3)
CALL CALPLT(HALF,O.,2)
CALL CALPLT(O.,-HALF,3)
CALL CALPLT(O.,HALF,2)
CALL CALPLT(O.,O.,3)
XCOR(NPLOT+1)=0.
XCOR(NPLOT+2)=SCALE
YCOR(NPLOT+1)=0.
YCOR(NPLOT+2)=SCALE
CALL LINPLT(XCCOR,YCCCR,NPLCT,1,NSKIPS,NSYMB,NSIZES,0)
IF(NSKIPS.LT.0) GO TO 5
STX=XCOR(NPLOT)
STY=YCOR(NPLOT)
STX1=XCOR(1)
STY1=YCOR(1)
CALL CALPLT(STX,STY,3)
CALL CALPLT(STX1,STY1,2)
5 CONTINUE
HGT=0.015*HPAT
XSC=-HALF
YSC=-HALF-0.07*HPAT
IF(IUNITS.EQ.2) GO TO 6
CALL NOTATE(XSC,YSC,HGT,15HSCALE, CM/IN = ,0.,15)
XSC=XSC+(90./7.)*HGT
GO TO 7
6 CALL NOTATE(XSC,YSC,HGT,16HSCALE, WVL/IN = ,0.,16)
XSC=XSC+(96./7.)*HGT
7 CALL NUMBER(XSC,YSC,HGT,SCALE,O.,4)
CALL CALPLT(O.,O.,3)
XNEW=0.8*HPAT
YNEW=0.
RETURN
305 FORMAT(2SH +++++++ KNTPLT= I3)
END

```

APPENDIX A – Continued

Subroutine DBPLOT

SUBROUTINE DBPLOT(HPAT,KI,ISKIPP,ISIZEP,
1 THTA,AEPH1,AEY,PEPH1)

```

C ****
C *
C * PURPOSE TO USE CALCCMP EQUIPMENT TO PLOT MAGNITUDE AND PHASE *
C * VARIATIONS OF A SINGLE COMPONENT OF THE RADIATION *
C * FIELD AS A FUNCTION OF ANGLE *
C *
C * INPUT DATA HPAT=5.* (RADIUS OF POLAR PLOT, INCHES) *
C * FOR TYPE 400 PAPER, (HPAT.LE.10.) *
C * FOR TYPE 300 PAPER, (HPAT.LE.28.) *
C * TO OBTAIN POLAR PLOTS IDENTICAL TO PATTERN *
C * RECORDER POLAR PLOTS, USE HPAT=18.75 *
C * KI=NUMBER OF POINTS TO BE PLOTTED *
C * ISKIPP=1 FOR SYMBOL EVERY DATA POINT, *
C * 2 FOR SYMBOL EVERY OTHER DATA POINT, ETC. *
C * ISIZEP=1 FOR SMALLEST SIZE SYMBOL, 2 FOR MEDIUM *
C * SIZE SYMBOL, AND 3 FOR LARGEST SIZE SYMBOL *
C * THTA=ARRAY CONTAINING THE ANGULAR VALUES (DEGREES) *
C * FOR WHICH THE FIELD IS TO BE PLOTTED. FOR A *
C * COMPLETE POLAR PLOT, THTA(1)=0., THTA(KI)=360. *
C * AEPH1=ARRAY OF MAGNITUDE VALUES (DB) CORRESPONDING *
C * TO ANGULAR VALUES IN THTA ARRAY. VALUES *
C * MUST LIE BETWEEN 0 DB (MAX) AND -40 DB (MIN) *
C * PEPH1=ARRAY OF PHASE VALUES (DEGREES) CORRESPONDING *
C * TO ANGULAR VALUES IN THTA ARRAY. VALUES *
C * MUST LIE BETWEEN 180. (MAX) AND -180. (MIN) *
C *
C * AEY IS AN ARRAY USED FOR INTERMEDIATE CALCULATIONS *
C *
C * RESTRICTIONS THE ARRAYS THTA, AEPH1, PEPH1, AND AEY MUST *
C * BE DIMENSIONED AT LEAST AS LARGE AS THE VALUE *
C * (KI+2) IN THE CALLING PROGRAM. COMMON /BLK1/
C * KNTPLT,XNEW,YNEW MUST ALSO APPEAR IN CALLING *
C * PROGRAM *
C *
C ****
C
COMMON /BLK1/ KNTPLT,XNEW,YNEW
DIMENSION THTA(1),AEPH1(1),AEY(1),PEPH1(1)
PI=3.141592653589793
RDW=PI/180.
KNTPLT=KNTPLT+1
WRITE(6,305) KNTPLT
IF(KNTPLT.EQ.1) GO TO 191
CALL CALPLT(XNEW,YNEW,-3)
191 CONTINUE
STX=0.2075*HPAT
STY=0.00375*HPAT
STH=0.015*HPAT
CALL NUMBER(STX,STY,STH,C.,0.,-1)
STX1=STX+0.0128*HPAT
STY1=STY+0.010*HPAT
STH1=0.006*HPAT
CALL NUMBER(STX1,STY1,STH1,C.,0.,-1)
STY=-0.01875*HPAT
CALL NUMBER(STX,STY,STH, 360.,0.,-1)
STX1=STX+0.03857*HPAT
STY1=STY+0.010*HPAT

```

APPENDIX A - Continued

```

CALL NUMBER(STX1,STY1,STH1,0.,0.,-1)
STX=-0.01071*HPAT
STY=0.2075*HPAT
CALL NUMBER(STX,STY,STH,90.,0.,-1)
STA1=STX+0.02571*HPAT
STY1=STY+0.010*HPAT
CALL NUMBER(STX1,STY1,STH1,0.,0.,-1)
STA=-0.2495*HPAT
STY=-0.0075*HPAT
CALL NUMBER(STX,STY,STH,180.,0.,-1)
STA1=STX+0.03857*HPAT
STY1=STY+0.010*HPAT
CALL NUMBER(STX1,STY1,STH1,0.,0.,-1)
STA=-0.01714*HPAT
STY=-0.2225*HPAT
CALL NUMBER(STX,STY,STH,270.,0.,-1)
STA1=STX+0.03857*HPAT
STY1=STY+0.010*HPAT
CALL NUMBER(STX1,STY1,STH1,0.,0.,-1)
SRHOU=25.
SRHO=SRHOU*RDN
SRAD=0.2025*HPAT
STA=-SRAD*SIN(SRHC)
STY=SRAD*COS(SRHO)
CALL NUMBER(STX,STY,STH,0.,SRHOU,-1)
CALL NOTATE(STX,STY,STH,4H DB,SRHOU,4)
SRAD=0.1525*HPAT
STA=-SRAD*SIN(SRHO)
STY=SRAD*COS(SRHO)
CALL NUMBER(STX,STY,STH,-10.,SRHOU,-1)
SRAD=0.1025*HPAT
STX=-SRAD*SIN(SRHC)
STY=SRAD*COS(SRHO)
CALL NUMBER(STX,STY,STH,-20.,SRHOU,-1)
SRAD=0.0525*HPAT
STX=-SRAD*SIN(SRHC)
STY=SRAD*COS(SRHC)
CALL NUMBLR(STX,STY,STH,-30.,SRHOU,-1)
HRAD=0.2*HPAT
CALL CALPLT(HRAD,0.,3)
LEND=6
DSRH0=PI/FLOAT(LEND)
DO 195 L=1,LEND
LM1=L-1
DSRH01=DSRH0*FLCAT(LM1)
SX1=HRAD*COS(DSRH01)
SY1=HRAD*SIN(DSRH01)
CALL CALPLT(-SX1,-SY1,2)
DSRH02=DSRH0*FLCAT(L)
SX2=HRAD*COS(DSRH02)
SY2=HRAD*SIN(DSRH02)
CALL CALPLT(SX2,SY2,3)
193 CONTINUE
CALL CALPLT(0.,0.,3)
KEND=4
SURD=HRAD/FLOAT(KEND)
DO 195 K=1,KEND
XX0=SURD*FLOAT(K)
CALL CIRCLE(XX0,0.,0.,360.,XX0,XX0,3)
195 CONTINUE

```

APPENDIX A – Continued

```

DBPIN=200./HPAT
DO 221 KX=1,KI
THTA1=THTA(KX)*RDN
AEPH2=AEPH1(KX)+40.
AEPH1(KX)=(AEPH2/DBPIN)*COS(THTA1)
AEY(KX)=(AEPH2/DBPIN)*SIN(THTA1)
221 CONTINUE
AEPH1(KI+1)=0.
AEPH1(KI+2)=1.
AEY(KI+1)=0.
AEY(KI+2)=1.
CALL LINPLT(AEPH1,AEY,KI,1,ISKIPP,1,ISIZEP,C)
XNEW=-0.2*HPAT
YNEW=-0.52*HPAT
KNTPLT=KNTPLT+1
WRITE(6,305) KNTPLT
CALL CALPLT(XNEW,YNEW,-3)
USTCE=0.4*HPAT
DUVV1=360./USTCE
XTMAJ=0.25*USTCE
XTMIN=XTMAJ/9.
STH=0.02*HPAT
CALL AXES(0.,0.,0.,USTCE,0.,DUVV1,XTMAJ,XTMIN,14HTHETA, DEGREES,
1 STH,-14)
USTCE=0.3*HPAT
DUVV2=360./USTCE
XTMAJ=0.25*USTCE
XTMIN=XTMAJ/9.
CALL AXES(0.,0.,90.,USTCE,-180.,DUVV2,XTMAJ,XTMIN,
1 14HPHASE, DEGREES,STH,14)
XSGRD=(0.4*HPAT)/12.
YSGRD=(0.3*HPAT)/4.
CALL GRID(0.,0.,XSGRD,YSGRD,12,4)
THTA(KI+1)=0.
THTA(KI+2)=DUVV1
PEPH1(KI+1)=-180.
PEPH1(KI+2)=DUVV2
CALL LINPLT(THTA,PEPH1,KI,1,ISKIPP,1,ISIZEP,0)
XNEW=0.8*HPAT
YNEW=0.62*HPAT
RETURN
305 FORMAT(25H +++++++ KNTPLT= 13)
END

```

APPENDIX B

NUMERICAL EXAMPLE

The purpose of this appendix is to present a numerical example which illustrates the application of the digital computer programs presented and described in appendix A. The example is the computation of the roll-plane radiation patterns for case 3. In the example, the frequency range is the interval of 5.250 GHz to 14.000 GHz, with an increment of 1.750 GHz. Consequently, FMCO = 5250., FMCD = 1750., and FMCF = 14000. The two annular slots for case 3 require four equivalent narrow axial slots; consequently, NPORT = 4.

The cross-section profile, shown in figure 8, is initially described, as shown in figure 13, by 55 coarse points; thus, NPTIN = 55. In figure 13, the numbers between any two consecutive points specify the number of segments to occur between the two points by subroutines SPLFIT and SPFIT2. As noted in appendix A, the number of points generated between a pair of consecutive points is one less than the number of segments that occur. In figure 13, coarse point 27 appears to lie in an approximately linear region of the profile; consequently, point 27 is chosen as the point for initiation of the spline fit procedure; that is, ISTART = 27. Other input data for the example are that MADM = 0, KI = 361, KWRT1 = 1, KWRT2 = 1, KWRT3 = 1, ISKIPP = 15, ISIZEP = 1, and HPAT = 18.75.

Input Data Cards

A listing of the input data cards for the numerical example is on the following page. The first card contains, in sequence, the values NPTIN, ISTART, NPORT, MADM, KI, KWRT1, KWRT2, KWRT3, ISKIPP, ISIZEP, HPAT, FMCO, FMCD, and FMCF.

The next four cards are cards which specify the port index I, the coarse point index JVGS(I), and the complex voltage strength VGS(I) for each of the four equivalent narrow axial slots which excite the configuration. The first two cards apply for the annular slot located at B₁ (see figs. 1 and 8) and the second two cards apply for the annular slot located at B₂.

The next 55 cards specify identifying integers and the X- and Y-coordinates, in cm, of the 55 coarse points. The first of these cards is for coarse point 1, the second for coarse point 2, and so forth. In particular, on the Ith card are the identifying integer IGNORE, the X-coordinate PNTIN(I,1) in cm, and the Y-coordinate PNTIN(I,2) in cm of the Ith coarse point.

APPENDIX B – Continued

Execution

After the input data cards are read by the main program, execution occurs. The printer output data follow:

```
*****  
NPTIN=55    ISTART=27  
  
IDIVL ARRAY VALUES  
3 1 1 1 1 1 1 1 3 6 4 4 4 4 4 4 4 4 4 4 4 4 4 6 3 1 1 1 1 1 1 1 3 7 3 3 3  
3 4 4 4 4 4 4 4 3 3 3 3 7  
  
NPOINT   MXNPT   NPORT  MXPORT     MAUM      KI    KWRT1    KWRT2    KWRT3  ISKIPP  ISIZEP   HPAT    FMCD    FMCD    FMCF  
165      170       6       4        0      361      1       1       1       15      1   18.75  5250.0  1750.C14000.0  
  
*****+ KNTPLT= 1  
LOCATION OF POINTS  
POINT      X, CM.      Y, CM.  
1          9.6100      0.0000  
2          9.5365      .2658  
3          9.4620      .5313  
4          9.3880      .7970  
5          9.3690      .8660  
6          9.3500      .9340  
7          9.2570      1.2680  
8          9.1650      1.0000  
9          9.0730      1.9320  
10         9.9800      2.2660  
11         8.9610      2.3340  
12         8.9420      2.4030  
13         8.8683      2.6887  
14         8.7940      2.9343  
15         8.7200      3.2000  
16         8.5832      3.7627  
17         8.4487      4.2060  
18         8.3137      4.7692  
19         8.1757      5.2114  
20         8.0320      5.7120  
21         7.8800      6.2100  
22         7.7232      6.6879  
23         7.5562      7.1625  
24         7.3785      7.6333  
25         7.1903      8.1000  
26         6.9911      8.5602  
27         6.7794      9.0146  
28         6.5530      9.4617  
29         6.3100      9.9000  
30         6.0566      10.3104  
31         5.7866      10.7223  
32         5.5008      11.1171  
33         5.2000      11.5000  
34         4.9135      11.8387  
35         4.6163      12.1887  
36         4.3118      12.4518  
37         4.0000      12.8100  
38         3.6660      13.1350  
39         3.3213      13.4561  
40         2.9510      13.7526  
41         2.5800      14.0200  
42         2.2770      14.1970  
43         1.9614      14.3517  
44         1.6351      14.4679  
45         1.3000      14.6000  
46         .9802      14.6844  
47         .6559      14.7472  
48         .3287      14.7665  
49         0.0000      14.8000  
50         -0.3287     14.7665  
51         -0.6559     14.7472  
52         -0.9802     14.6844
```

APPENDIX B - Continued

53	-1.3003	14.6000
54	-1.6351	14.4879
55	-1.9614	14.3537
56	-2.2770	14.1976
57	-2.5800	14.0200
58	-2.9610	13.7526
59	-3.3213	13.4561
60	-3.6660	13.1390
61	-4.0000	12.8100
62	-4.3118	12.4918
63	-4.6169	12.1687
64	-4.9135	11.8387
65	-5.2000	11.5000
66	-5.5007	11.1171
67	-5.7865	10.7223
68	-6.0565	10.3163
69	-6.3103	9.9000
70	-6.5531	9.4617
71	-6.7797	9.0147
72	-6.9914	8.5603
73	-7.1900	8.1000
74	-7.3779	7.6331
75	-7.5551	7.1622
76	-7.7223	6.6876
77	-7.8800	6.2100
78	-8.0343	5.7127
79	-8.1808	5.2129
80	-8.3210	4.7114
81	-8.4565	4.2084
82	-8.5891	3.7044
83	-8.7200	3.2000
84	-8.7944	2.9345
85	-8.8685	2.6688
86	-8.9420	2.4030
87	-8.9610	2.3340
88	-8.9800	2.2680
89	-9.0730	1.9320
90	-9.1650	1.6000
91	-9.2570	1.2680
92	-9.3500	.9340
93	-9.3690	.8680
94	-9.3880	.7970
95	-9.4620	.5313
96	-9.5366	.2658
97	-9.6100	0.0000
98	-9.7302	-45e6
99	-9.8457	-9183
100	-9.9607	-1.3761
101	-10.0793	-1.8371
102	-10.2059	-2.2944
103	-10.3447	-2.7490
104	-10.5000	-3.2000
105	-10.6277	-3.5441
106	-10.7377	-3.8920
107	-10.8000	-4.1500
108	-10.7947	-4.5782
109	-10.7481	-4.9010
110	-10.6000	-5.2000
111	-10.3086	-5.5685
112	-9.9278	-5.8629
113	-9.5000	-6.1000
114	-9.0066	-6.5163
115	-8.5063	-6.4926
116	-8.0000	-6.0400
117	-7.5065	-6.7653
118	-7.0077	-6.8718
119	-6.5050	-6.9669
120	-6.0000	-7.0300
121	-5.5011	-7.1216
122	-5.0014	-7.1835
123	-4.5011	-7.2361
124	-4.0000	-7.2800
125	-3.5006	-7.3157
126	-3.0007	-7.3459
127	-2.5005	-7.3731
128	-2.0000	-7.4000
129	-1.5000	-7.4400
130	-1.0000	-7.4538
131	-5.0000	-7.4727
132	0.0000	-7.4800

APPENDIX B - Continued

133	.5000	-7.4727
134	1.0000	-7.4538
135	1.5000	-7.4250
136	2.0000	-7.4000
137	2.5005	-7.3751
138	3.0007	-7.3459
139	3.5006	-7.3157
140	4.0000	-7.2800
141	4.5011	-7.2351
142	5.0014	-7.1835
143	5.5011	-7.1214
144	6.0000	-7.0500
145	6.5050	-6.9669
146	7.0077	-6.8718
147	7.5065	-6.7623
148	8.0000	-6.6400
149	8.5068	-6.4926
150	9.0066	-6.3163
151	9.5000	-6.1000
152	9.9278	-5.8629
153	10.3086	-5.5685
154	10.6300	-5.2000
155	10.7281	-4.9010
156	10.7947	-4.5782
157	10.8030	-4.2500
158	10.7377	-3.8920
159	10.6277	-3.5441
160	10.5000	-3.2000
161	10.3447	-2.7450
162	10.2059	-2.2944
163	10.0793	-1.8371
164	9.9607	-1.3781
165	9.8457	-0.9182
166	9.7303	-0.4586

FREQUENCY = 5250.0 MHZ
WAVELENGTH = 5.71 CM.

***** KNTPLT = 2

NUMBER OF POINTS DESCRIBING THE CYLINDER=166

POINT	GEOMETRY OF CYLINDRICAL CROSS SECTION		DRIVING POINT VOLTAGES		
	X, WVL.	Y, WVL.	U, WVL.	RE(V), VOLTS	IM(V), VOLTS
1	1.6818	0.0000	.0483		
2	1.6689	.0465	.0483		
3	1.6559	.0930	.0483		
4	1.6429	.1395	.0125		
5	1.6396	.1516	.0124	1.0000	0.0000
6	1.6363	.1635	.0607		
7	1.6200	.2219	.0603		
8	1.6039	.2800	.0603		
9	1.5878	.3381	.0607		
10	1.5715	.3966	.0124		
11	1.5682	.4985	.0125		
12	1.5648	.4205	.0483		
13	1.5520	.4670	.0483		
14	1.5389	.5135	.0483		
15	1.5260	.5600	.0912		
16	1.5021	.6480	.0912		
17	1.4785	.7360	.0912		
18	1.4549	.8241	.0912		
19	1.4307	.9120	.0911		
20	1.4056	.9996	.0911		
21	1.3790	1.0868	.0880		
22	1.3516	1.1704	.0880		
23	1.3223	1.2534	.0881		
24	1.2912	1.3358	.0881		
25	1.2585	1.4175	.0877		
26	1.2234	1.4980	.0877		
27	1.1864	1.5776	.0877		
28	1.1468	1.6558	.0877		
29	1.1043	1.7325	.0853		
30	1.0599	1.8054	.0853		

APPENDIX B - Continued

31	1.0125	1.8764	.0853
32	.9624	1.9455	.0854
33	.9100	2.0125	.0776
34	.8599	2.0718	.0776
35	.8079	2.1295	.0778
36	.7546	2.1861	.0780
37	.7000	2.2417	.0821
38	.6415	2.2993	.0820
39	.5812	2.3543	.0817
40	.5182	2.4067	.0815
41	.4515	2.4535	.0815
42	.3985	2.4846	.0616
43	.3432	2.5119	.0617
44	.2861	2.5354	.0618
45	.2275	2.5550	.0579
46	.1715	2.5698	.0578
47	.1148	2.5808	.0577
48	.0575	2.5876	.0576
49	0.0000	2.5900	.0576
50	-.0575	2.5876	.0577
51	-.1148	2.5808	.0578
52	-.1715	2.5698	.0579
53	-.2275	2.5550	.0618
54	-.2861	2.5354	.0617
55	-.3432	2.5119	.0616
56	-.3985	2.4846	.0615
57	-.4515	2.4535	.0815
58	-.5182	2.4067	.0817
59	-.5812	2.3548	.0820
60	-.6415	2.2993	.0821
61	-.7000	2.2417	.0760
62	-.7546	2.1861	.0776
63	-.8079	2.1295	.0776
64	-.8599	2.0718	.0776
65	-.9100	2.0125	.0852
66	-.9624	1.9455	.0853
67	-1.0125	1.8764	.0853
68	-1.0599	1.8054	.0853
69	-1.1043	1.7325	.0877
70	-1.1458	1.6558	.0877
71	-1.1864	1.5776	.0877
72	-1.2235	1.4980	.0877
73	-1.2583	1.4175	.0881
74	-1.2911	1.3358	.0881
75	-1.3221	1.2534	.0880
76	-1.3514	1.1703	.0880
77	-1.3790	1.0868	.0911
78	-1.4060	.9997	.0911
79	-1.4316	.9123	.0911
80	-1.4562	.8245	.0912
81	-1.4799	.7365	.0912
82	-1.5031	.6483	.0912
83	-1.5260	.5600	.0483
84	-1.5390	.5135	.0483
85	-1.5520	.4670	.0483
86	-1.5648	.4205	.0125
87	-1.5682	.4085	.0124
88	-1.5715	.3966	.0607
89	-1.5878	.3581	.0603
90	-1.6039	.2600	.0603
91	-1.6200	.2219	.0607
92	-1.6363	.1635	.0124
93	-1.6396	.1516	.0125
94	-1.6429	.1395	.0483
95	-1.6559	.0930	.0483
96	-1.6689	.0465	.0483
97	-1.6818	0.0000	.0830
98	-1.7028	-.0803	.0829
99	-1.7230	-.1537	.0829
100	-1.7431	-.2512	.0830
101	-1.7639	-.3215	.0830
102	-1.7860	-.4015	.0832
103	-1.8103	-.4811	.0835
104	-1.8375	-.5600	.0642
105	-1.8598	-.6202	.0638
106	-1.8791	-.6811	.0636
107	-1.8900	-.7438	.0574
108	-1.8891	-.8012	.0577
109	-1.8774	-.8577	.0509
110	-1.8550	-.9100	.0822

-1.0000 0.0000

1.0000 0.0000

APPENDIX B – Concluded

SHORT-CIRCUIT ADMITTANCE MATRIX

POINT	PURT	POINT	PORT	G, MILLIMHOS	B, MILLIMHOS
5	1	5	1	0.00000000	0.00000000
5	1	11	2	0.00000000	0.00000000
5	1	87	3	0.00000000	0.00000000
5	1	93	4	0.00000000	0.00000000
11	2	5	1	0.00000000	0.00000000
11	2	11	2	0.00000000	0.00000000
11	2	87	3	0.00000000	0.00000000
11	2	93	4	0.00000000	0.00000000
87	3	5	1	0.00000000	0.00000000
87	3	11	2	0.00000000	0.00000000
87	3	87	3	0.00000000	0.00000000
87	3	93	4	0.00000000	0.00000000
93	4	5	1	0.00000000	0.00000000
93	4	11	2	0.00000000	0.00000000
93	4	87	3	0.00000000	0.00000000
93	4	93	4	0.00000000	0.00000000

On output, the input data, except for the 55 cards giving the coarse point X- and Y-coordinates, are printed first. Then, the indices and the X- and Y-coordinates of the 166 actual points generated by subroutines SPLFIT and SPFIT2 and required by subroutine TESLOT are printed in units of centimeters. The statement KNPLT = 1 implies that subroutine SKETCH has made a plot of these points and has given the scale factor below the plot in cm/inch (on the plotting paper).

Next, computations and plots as functions of frequency are made. The printer output is given only for the first frequency, 5.250 GHz. The printer output however is similar for all the remaining frequencies.

For a given frequency, the frequency and wavelength are written first, and a plot of the 166 points (KNPLT = 2) is made and the scale factor in wavelengths/inch on the plotting paper) is given below the plot. Next, a write out of the geometry of the cross section is given. In the write out, the X- and Y-coordinates are given in wavelengths at the specific frequency for a particular point, say, point I, and the length, in wavelengths, of the segment the end points of which are point I and point I + 1 is also given. The voltage strength of a narrow axial slot is also given at the point at which the slot is located.

Next, the computed radiation pattern is printed. In the program, PHI corresponds to ϕ_r of figures 1 and 8, and for a given value of PHI, the real part, the imaginary part, the magnitude, and the phase of the relative radiation field are printed.

Next, for a given value of PHI, the radiation field in decibels, the normalized radiation field, and the radiation field are printed. The statements KNPLT = 3 and KNPLT = 4 indicate that subroutine DBPLOT has made a radiation field magnitude polar plot and a radiation field phase rectangular plot, both plots of which are functions of ϕ_r . (See fig. 14.)

Finally, the short-circuit admittance matrix is printed. However, since MADM = 0, this part of the write out is meaningless.

REFERENCES

1. Harrington, Roger F.: Field Computation by Moment Methods. Macmillan Co., c.1968.
2. Harrington, Roger F.; and Mautz, Joseph R.: Theory of Characteristic Modes for Conducting Bodies. *IEEE Trans. Antennas & Propagation*, vol. AP-19, no. 5, Sept. 1971, pp. 622-628.
3. Harrington, Roger F.; and Mautz, Joseph R.: Computation of Characteristics Modes for Conducting Bodies. *IEEE Trans. Antennas & Propagation*, vol. AP-19, no. 5, Sept. 1971, pp. 629-639.
4. Richmond, J. H.: Computer Analysis of Three-Dimensional Wire Antennas. Tech. Rep. 2708-4 (Contract No. DAAD 05-69-C-0031), Dep. Elec. Eng., Ohio State Univ., Dec. 22, 1969.
5. Richmond, J. H.: An Integral-Equation Solution for TE Radiation and Scattering From Conducting Cylinders. NASA CR-2245, 1973.
6. Keller, Joseph B.: Geometrical Theory of Diffraction. *J. Opt. Soc. Amer.*, vol. 52, no. 2, Feb. 1962, pp. 116-130.
7. Kouyoumjian, Robert G.: Asymptotic High-Frequency Methods. *Proceedings IEEE*, vol. 53, no. 8, Aug. 1965, pp. 864-876.
8. Hutchins, David L.; and Kouyoumjian, Robert G.: Asymptotic Series Describing Time Diffraction of a Plane Wave by a Wedge. AFCRL-69-0412, U.S. Air Force, 1969. (Available from DDC as AD 699 228.)
9. Pathak, P. H.; and Kouyoumjian, R. G.: The Dyadic Diffraction Coefficient for a Perfectly Conducting Wedge. AFCRL-69-0546, U.S. Air Force, 1969. (Available from DDC as AD 707 827.)
10. Agrawal, Pradeep K.; Richards, George A.; Thiele, Gary A.; and Richmond, Jack H.: Analysis and Design of TEM-Line Antennas. *IEEE Trans. Antennas & Propagation*, vol. AP-20, no. 5, Sept. 1972, pp. 561-568.
11. Knepp, Dennis L.; and Goldhirsh, Julius: Numerical Analysis of Electromagnetic Radiation Properties of Smooth Conducting Bodies of Arbitrary Shape. *IEEE Trans. Antennas & Propagation*, vol. AP-20, no. 3, May 1972, pp. 383-388.
12. Goldhirsh, J.; Knepp, D. L.; Doviak, R. J.; and Unks, R.: Radiation From a Short Dipole or Monopole Near a Thick Conducting Cylinder of Resonant Length. *IEEE Trans. Antennas & Propagation*, vol. AP-19, no. 2, Mar. 1971, pp. 279-282.

13. Jones, J. Earl; Tsai, L. L.; Rudduck, R. C.; Swift, C. T.; and Burnside, W. D.: The Admittance of a Parallel-Plate Waveguide Aperture Illuminating a Metal Sheet. *IEEE Trans. Antennas & Propagation*, vol. AP-16, no. 5, Sept. 1968, pp. 528-535.
14. Balanis, Constantine A.; and Peters, Leon, Jr.: Aperture Radiation From an Axially Slotted Elliptical Conducting Cylinder Using Geometrical Theory of Diffraction. *IEEE Trans. Antennas & Propagation*, vol. AP-17, no. 4, July 1969, pp. 507-513.
15. Balanis, Constantine A.: Analysis of an Array of Line Sources Above a Finite Ground Plane. *IEEE Trans. Antennas & Propagation*, vol. AP-19, no. 2, Mar. 1971, pp. 181-185.
16. Burnside, Walter Dennis: Analysis of On-Aircraft Antenna Patterns. Tech. Rep. 3390-1 (Contract N62269-72-C-0354), Dep. Elec. Eng., Ohio State Univ., Aug. 1972.
17. Tsai, Leonard L.; Wilton, Donald R.; Harrison, Michael G.; and Wright, Eddy H.: A Comparison of Geometrical Theory of Diffraction and Integral Equation Formulation for Analysis of Reflector Antennas. *IEEE Trans. Antennas & Propagation*, vol. AP-20, no. 6, Nov. 1972, pp. 705-712.
18. Jasik, Henry, ed.: *Antenna Engineering Handbook*. McGraw-Hill Book Co., Inc., 1961.

TABLE I.- GEOMETRY AND EXCITATION DATA FOR APPLICATION OF RIEF FOR COMPUTATIONS OF SPACE SHUTTLE ANNULAR SLOT RADIATION PATTERNS

[All linear dimensions are for 1/35-scale model]

Case	Figure	Perimeter, cm	Number of points and simultaneous equations	Coordinates x,y, cm, of center of annular slot	Phasor voltage strength, volts, and coordinates x,y, cm, of equivalent narrow axial slots
1	6	70.55	154	$A = (0., 14.690)$ at P_{43}	$A \begin{cases} V_{40} = 1 \angle 0^\circ & \text{at } P_{40} = (0.762, 14.690) \\ V_{46} = 1 \angle 180^\circ & \text{at } P_{46} = (-0.762, 14.690) \end{cases}$
2	7	70.58	159	$B_1 = (9.165, 1.600)$ at P_8	$B_1 \begin{cases} V_5 = 1 \angle 0^\circ & \text{at } P_5 = (9.369, 0.866) \\ V_{11} = 1 \angle 180^\circ & \text{at } P_{11} = (8.961, 2.334) \end{cases}$
3	8	70.58	166	$B_1 = (9.165, 1.600)$ at P_8	$B_1 \begin{cases} V_5 = 1 \angle 0^\circ & \text{at } P_5 = (9.369, 0.866) \\ V_{11} = 1 \angle 180^\circ & \text{at } P_{11} = (8.961, 2.334) \end{cases}$
				$B_2 = (-9.165, 1.600)$ at P_{90}	$B_2 \begin{cases} V_{87} = 1 \angle 180^\circ & \text{at } P_{87} = (-8.961, 2.334) \\ V_{93} = 1 \angle 0^\circ & \text{at } P_{93} = (-9.369, 0.866) \end{cases}$
4	11	142.86	178	$A = (0., 11.500)$ at P_{48}	$A \begin{cases} V_{45} = 1 \angle 180^\circ & \text{at } P_{45} = (0.741, 11.766) \\ V_{51} = 1 \angle 0^\circ & \text{at } P_{51} = (-0.741, 11.234) \end{cases}$

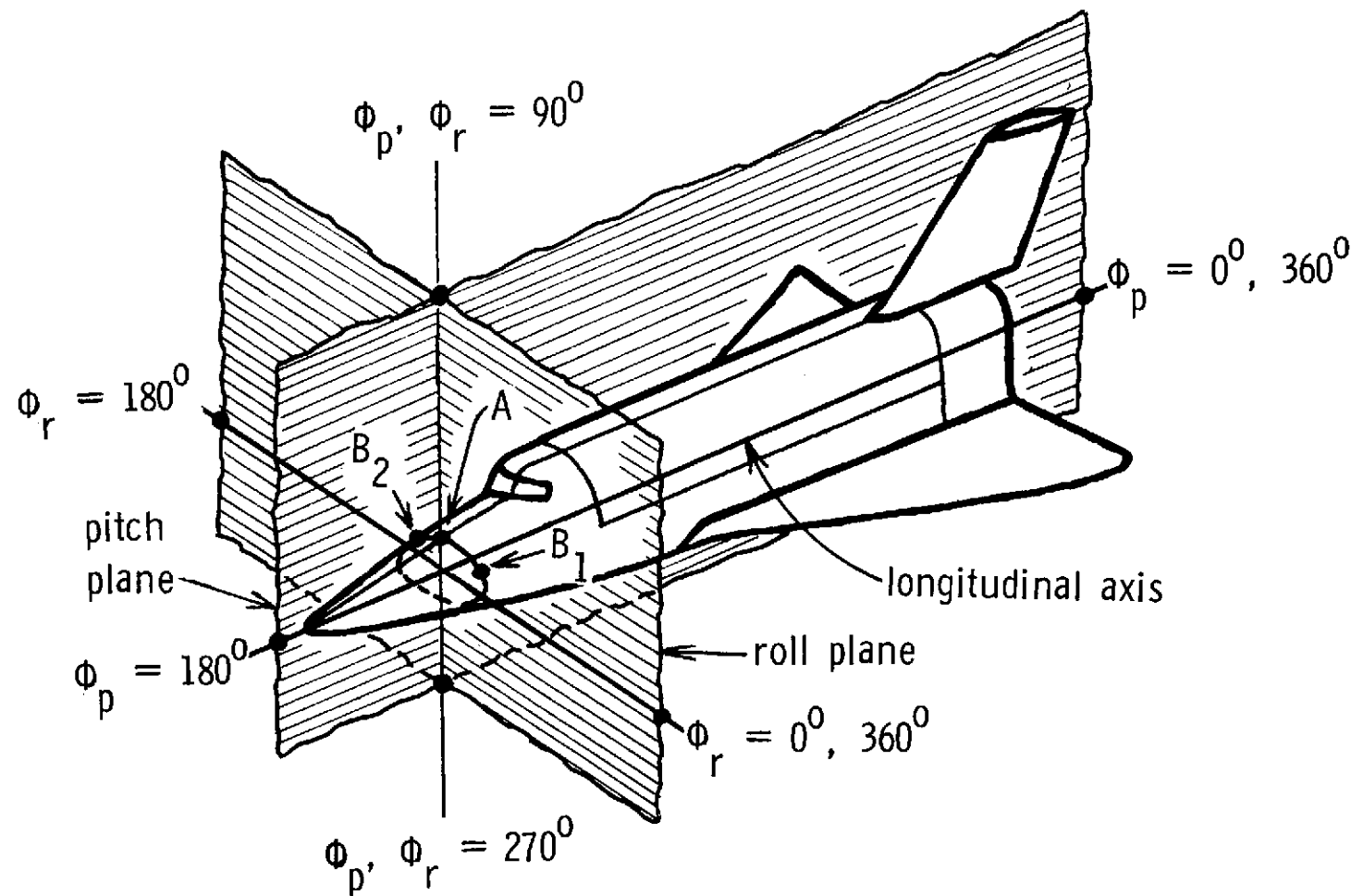


Figure 1.- Geometry of the Space Shuttle orbiter and location of the pitch and roll planes.

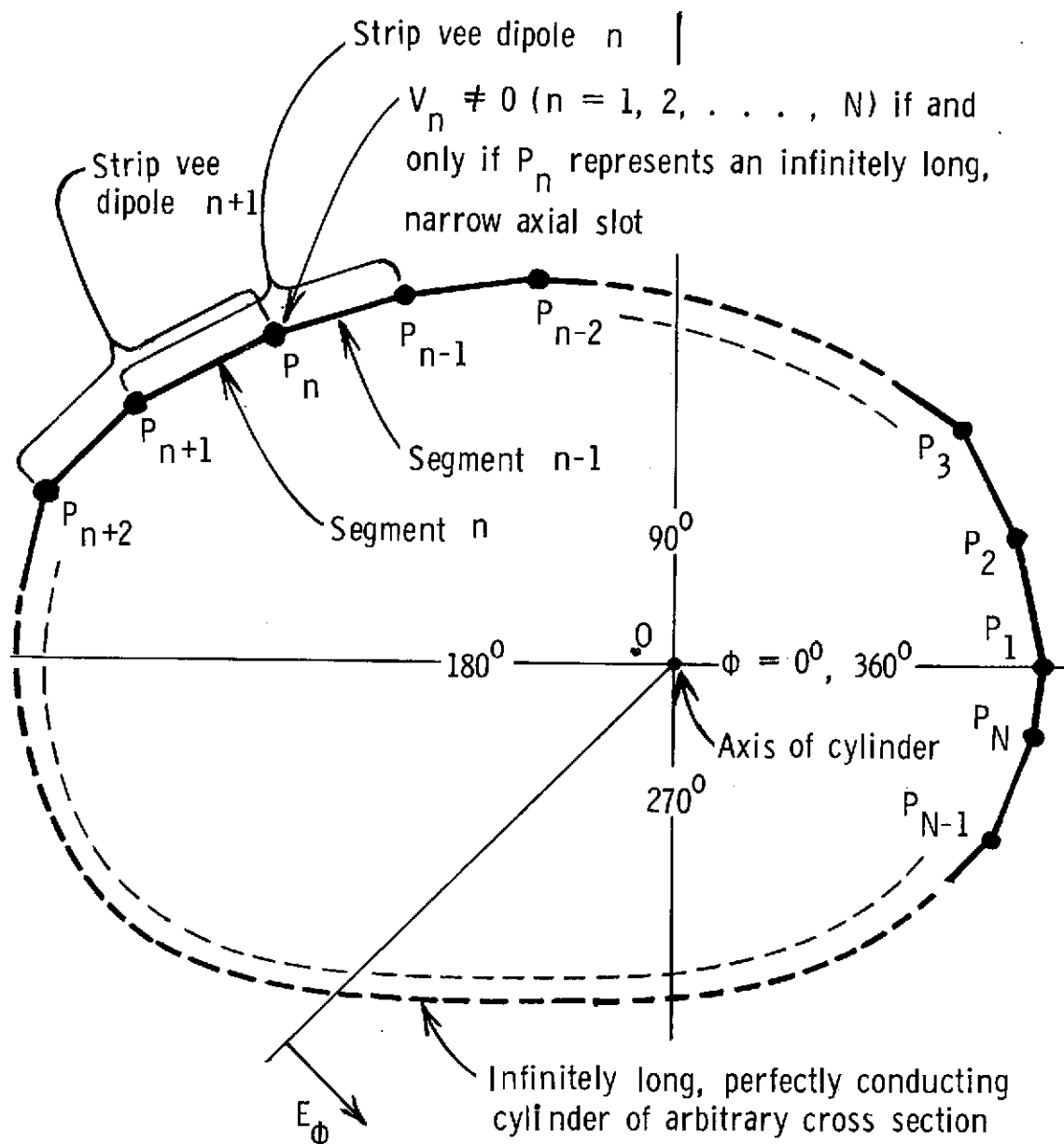


Figure 2.- Geometry for which RIEF is applicable.

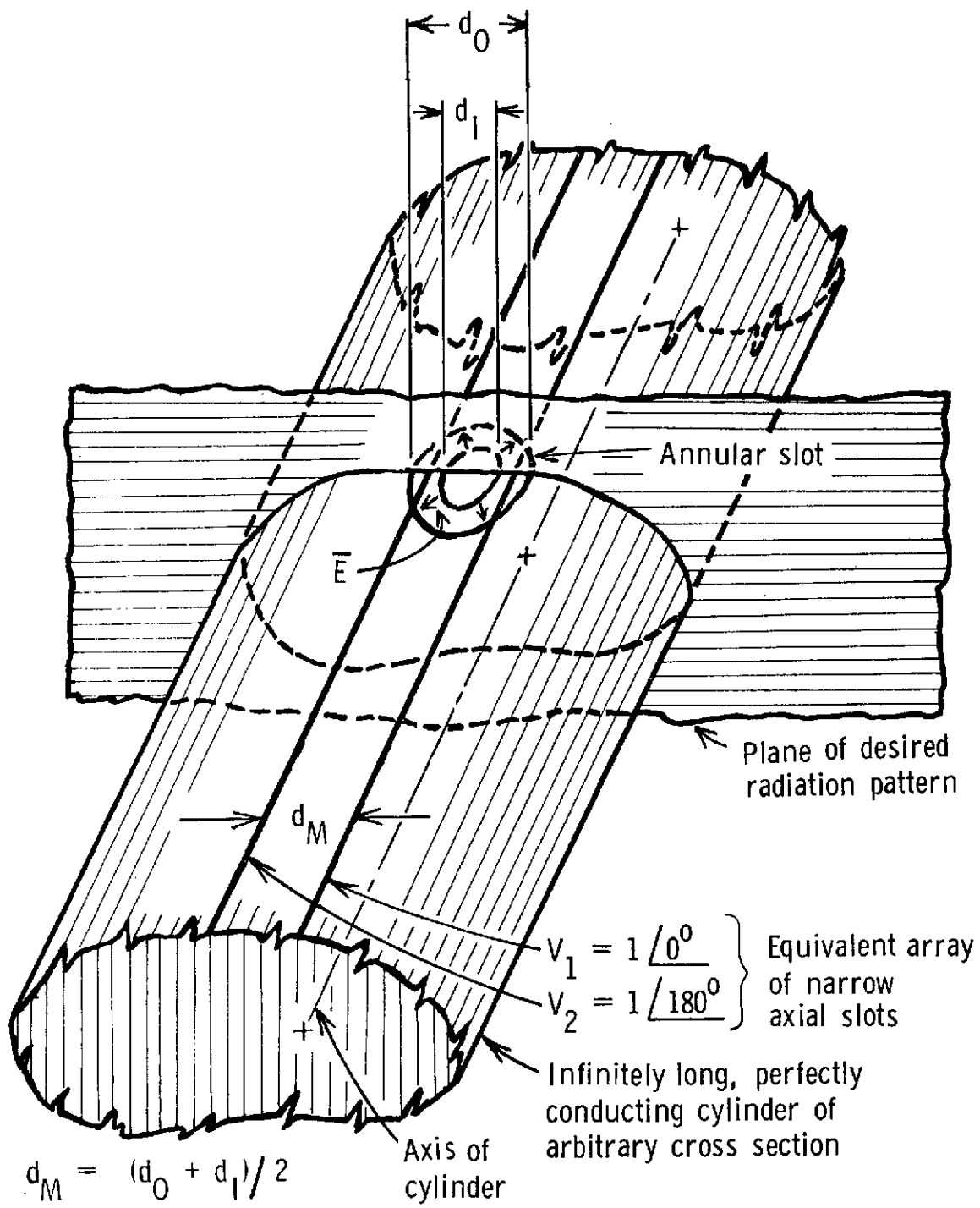
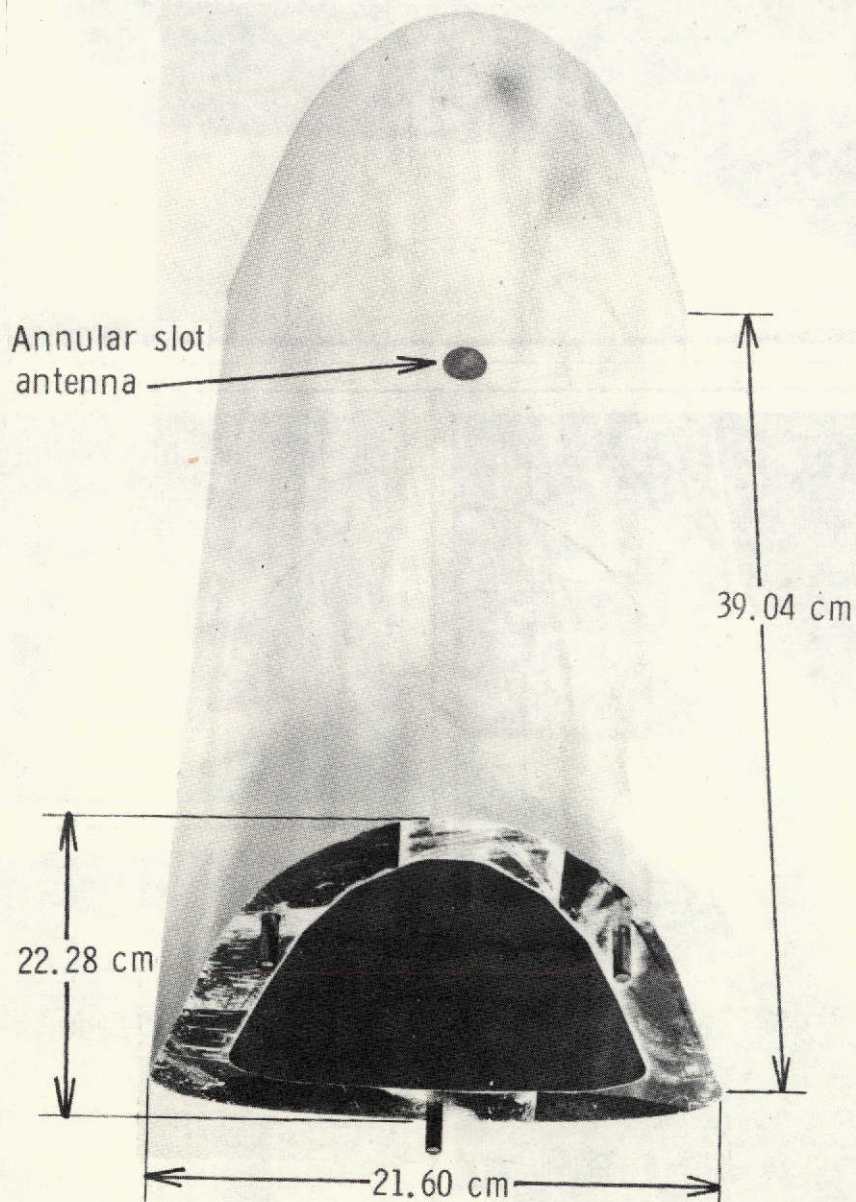
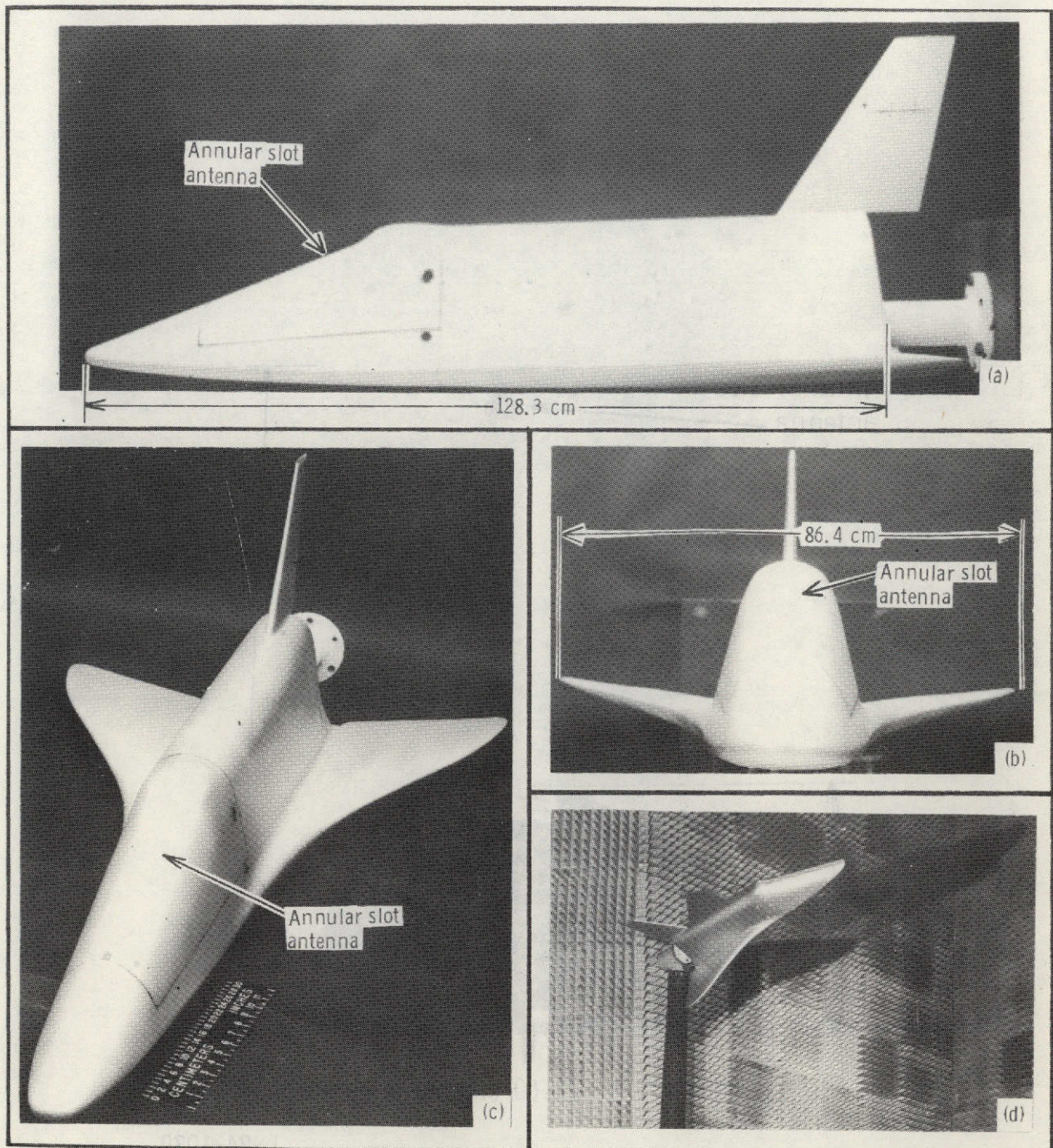


Figure 3.- Representation of an annular slot by an equivalent array of two narrow axial slots for purposes of computing the specified radiation pattern.



L-74-1070

Figure 4.- 1/35-scale model (cylindrical model) for obtaining roll-plane radiation patterns experimentally.



(a) Side view.

L-74-1071

(b) Front view.

(c) Oblique view.

(d) Model under test.

Figure 5.- 1/35-scale model (three-dimensional model) for obtaining roll- and pitch-plane radiation patterns experimentally.

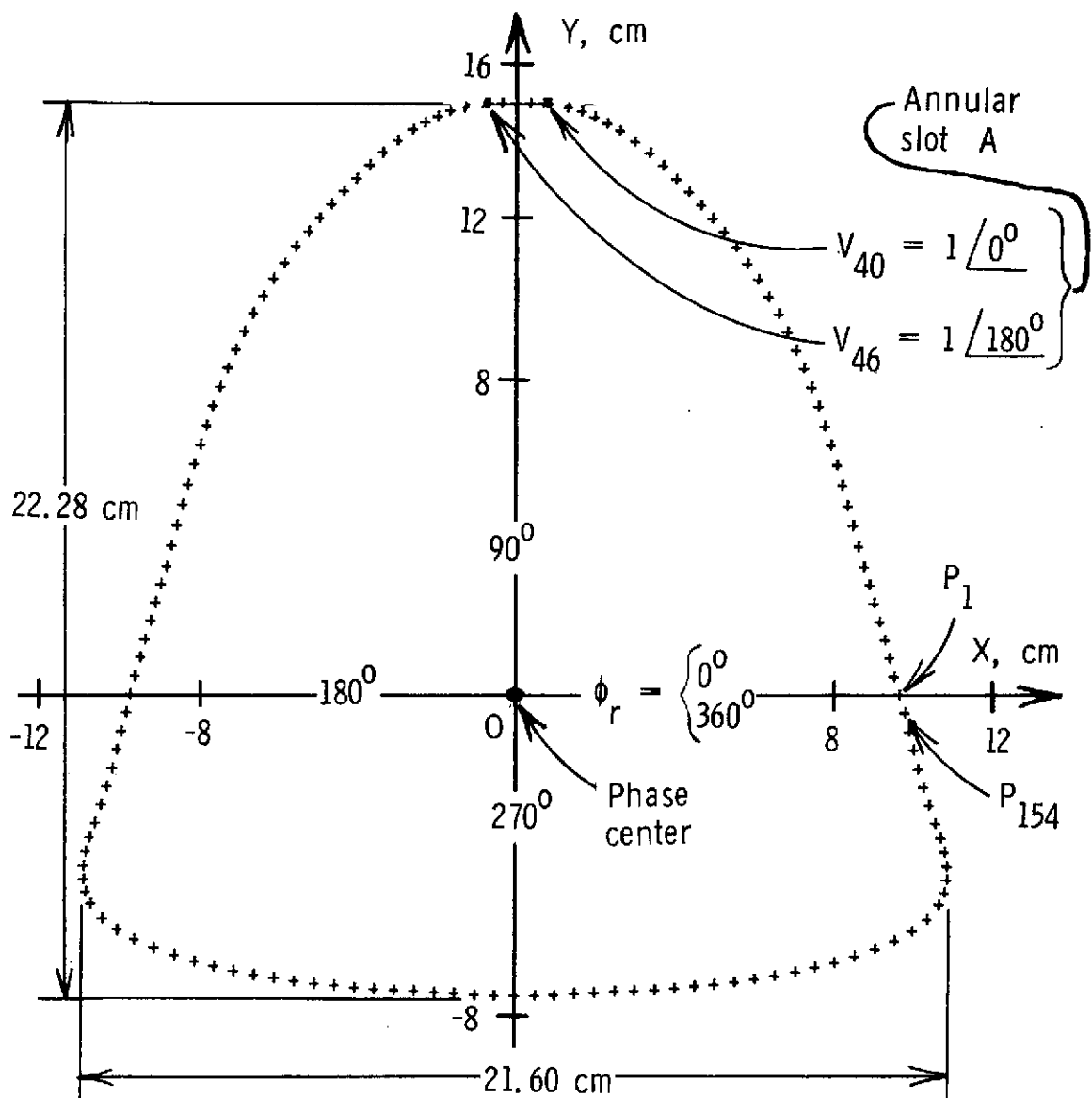


Figure 6.- Points describing roll-plane cross-section profile for case 1.

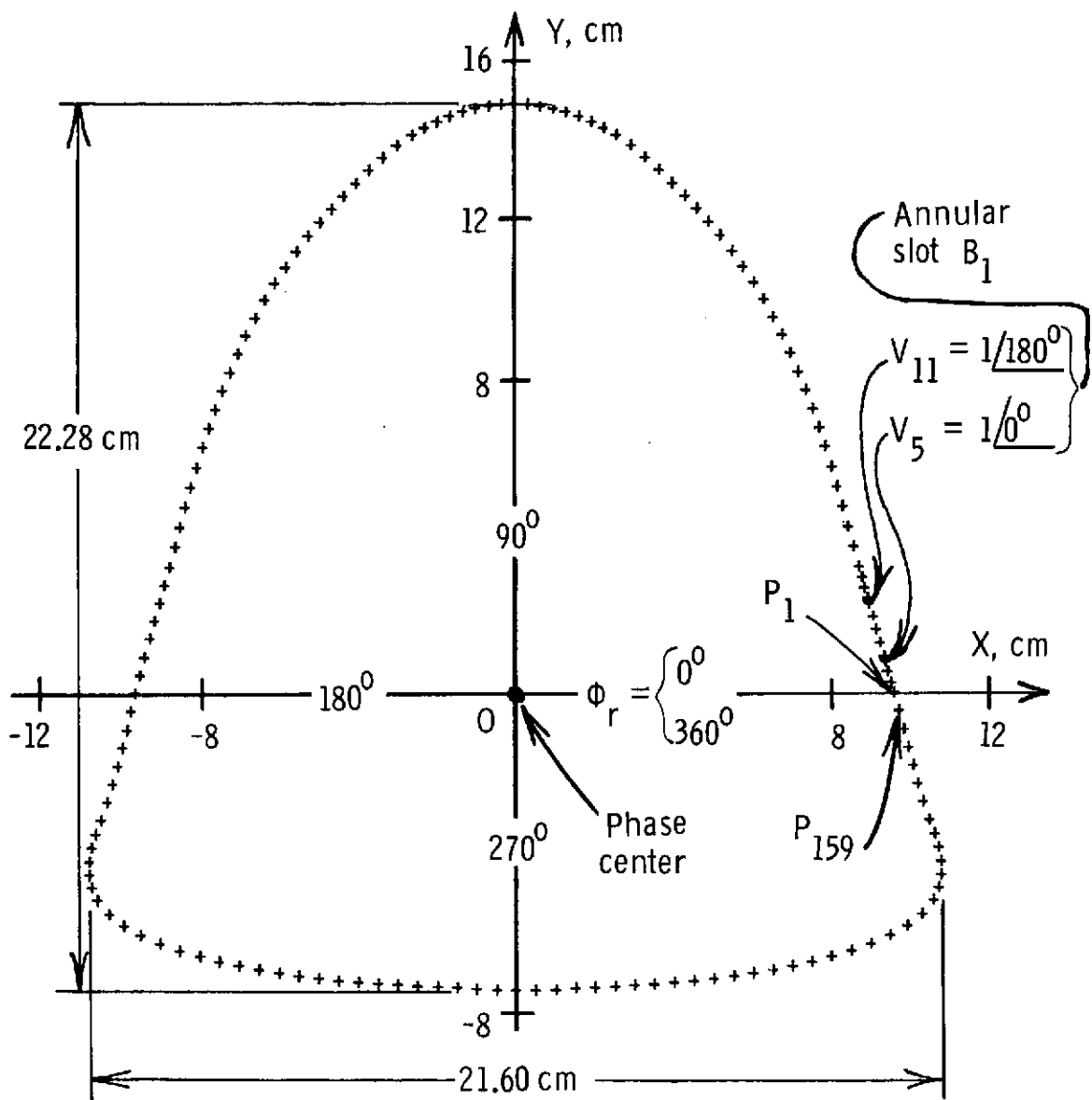


Figure 7.- Points describing roll-plane cross-section profile for case 2.

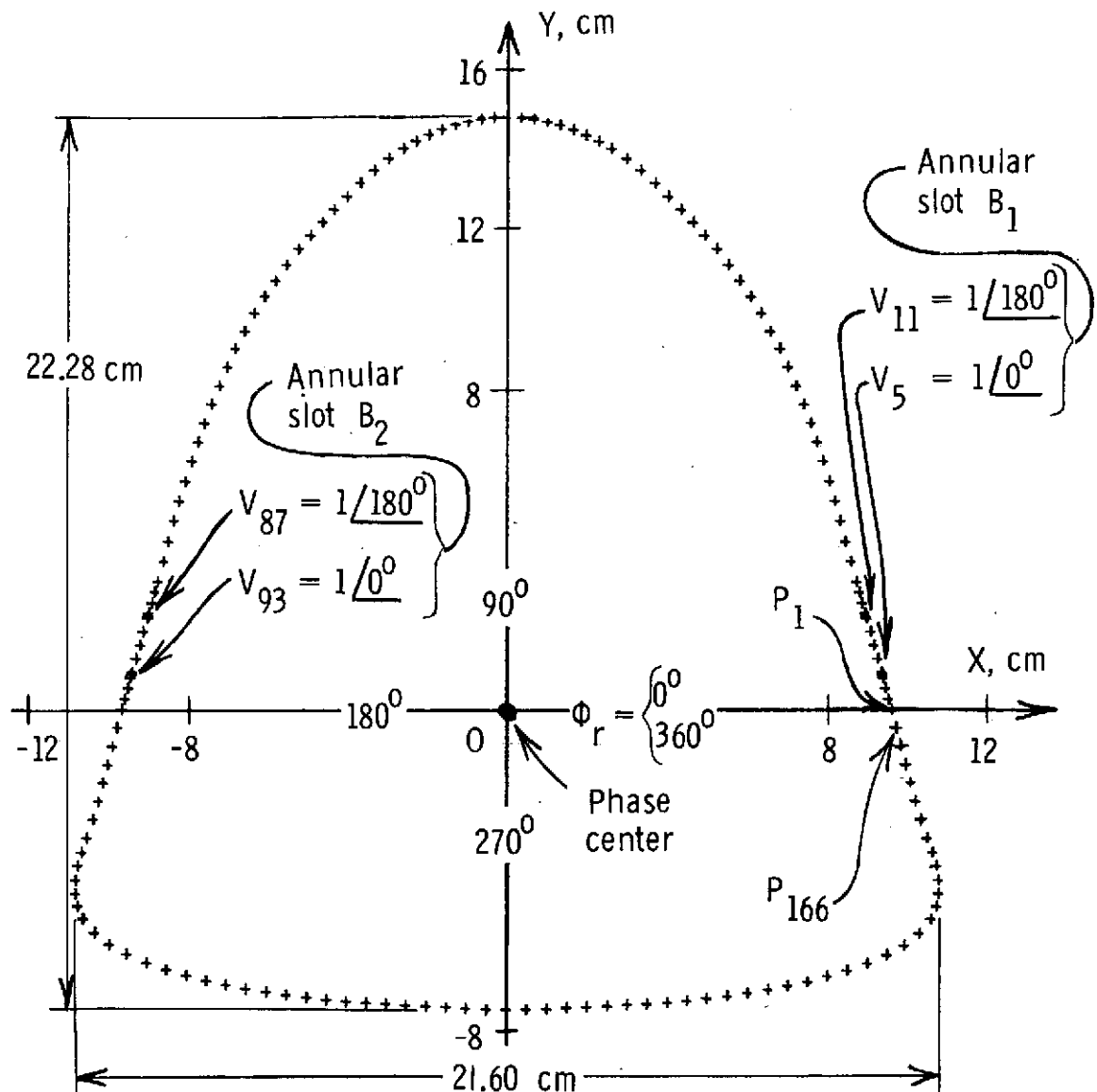


Figure 8.- Points describing roll-plane cross-section profile for case 3.

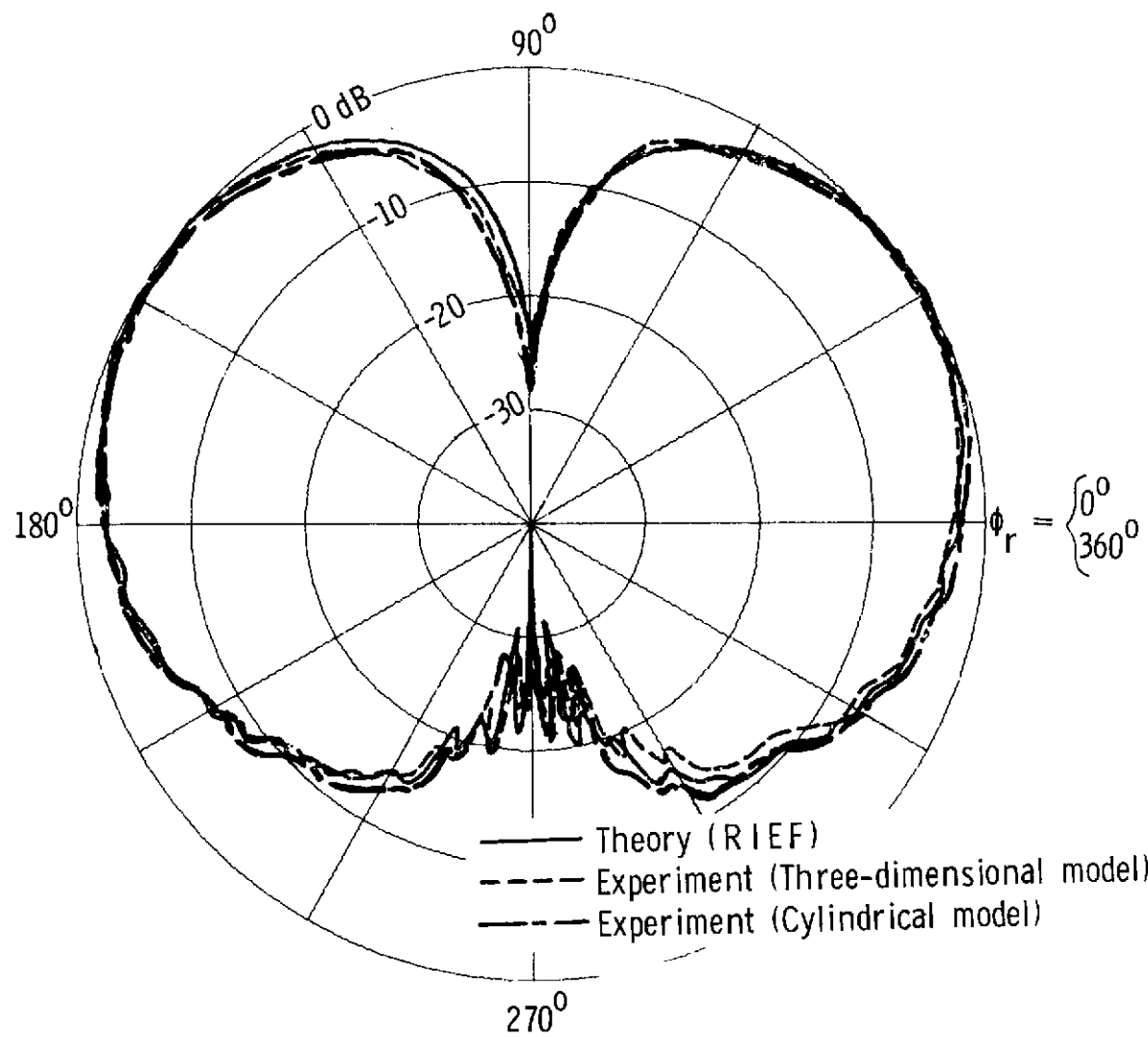


Figure 9.- Roll-plane radiation pattern for case 1 (theory compared with experiment).
 Frequency, 311.4 MHz (10.900 GHz).

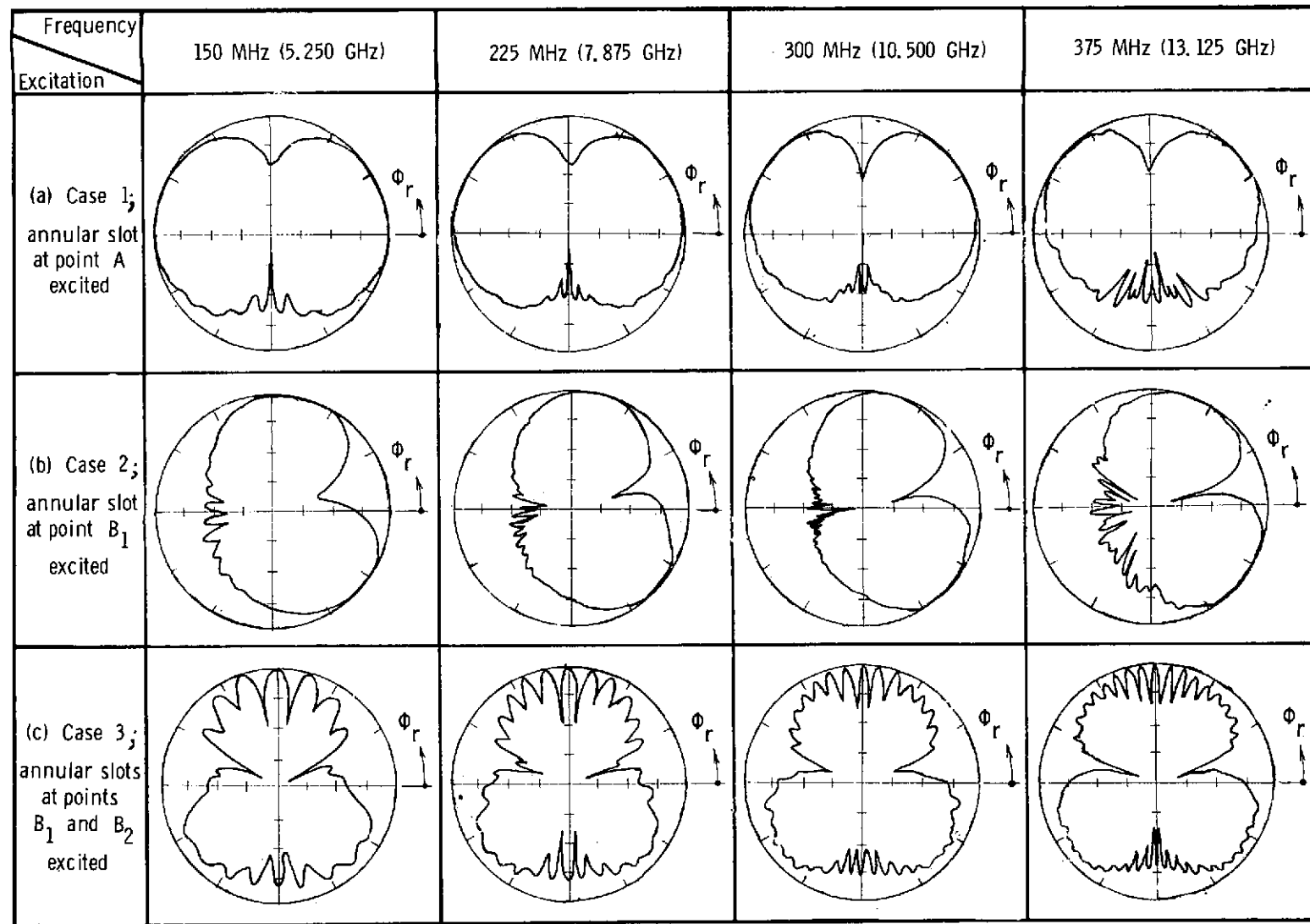


Figure 10.- Computed roll-plane radiation patterns as function of frequency.

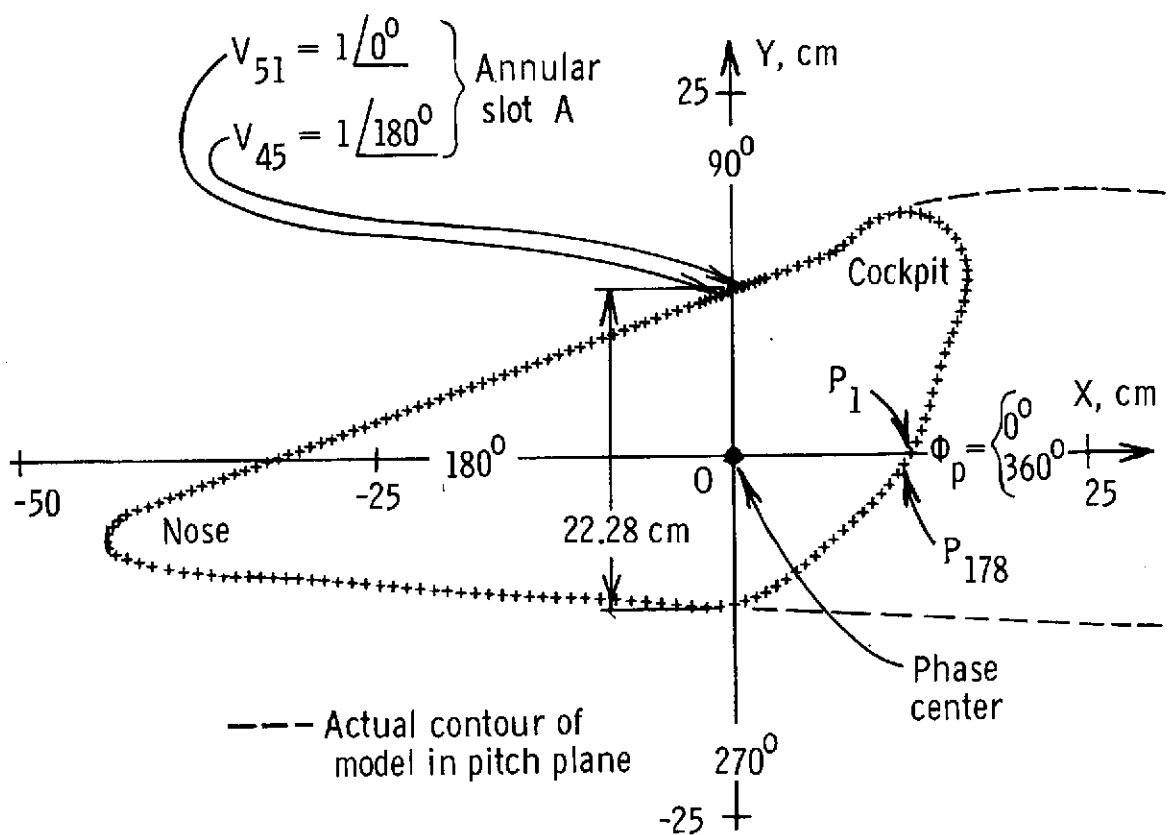


Figure 11.- Points describing pitch-plane cross-section profile for case 4.

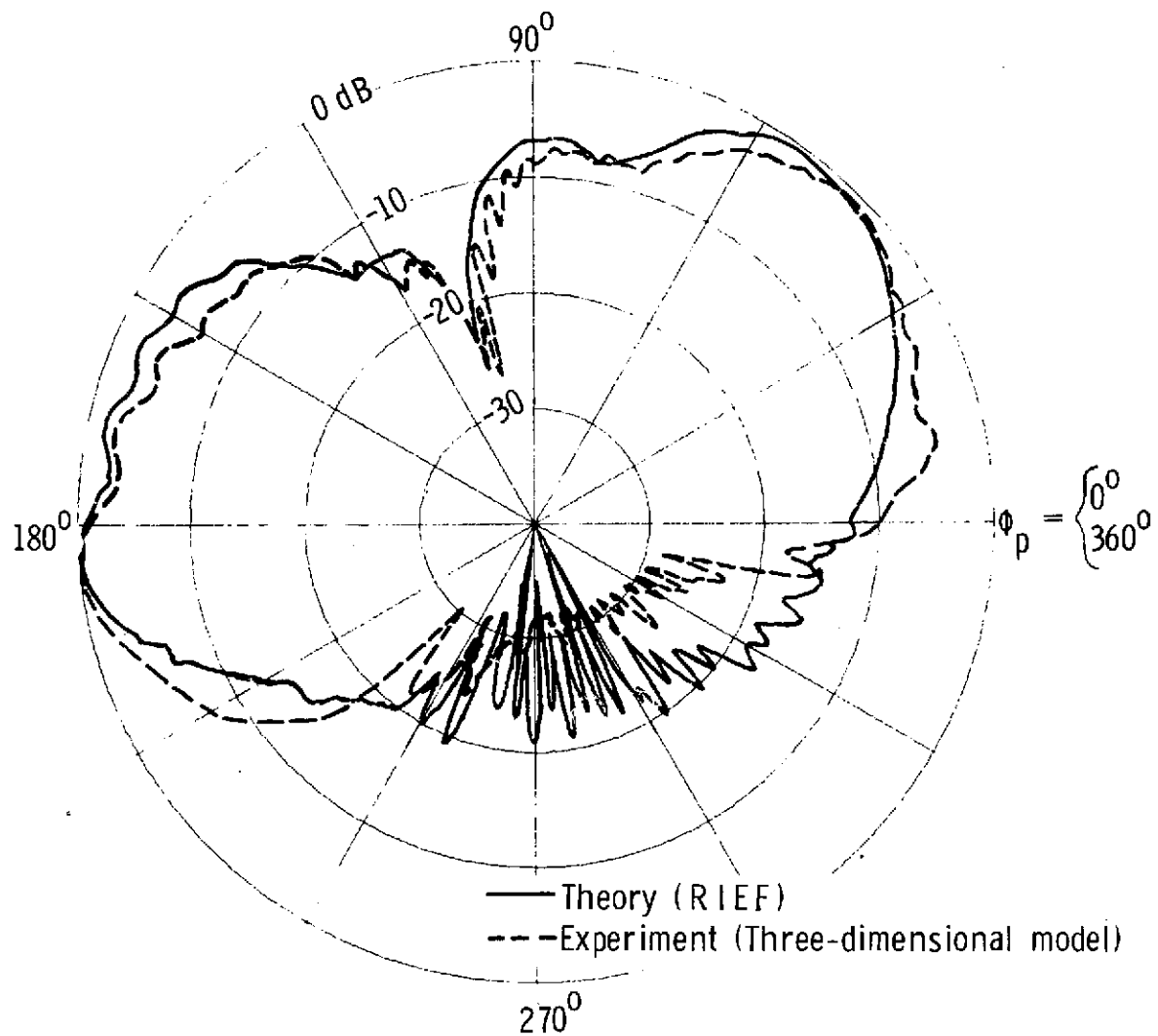


Figure 12.- Pitch-plane radiation pattern for case 4 (theory compared with experiment).
Frequency, 155.7 MHz (5.450 GHz).

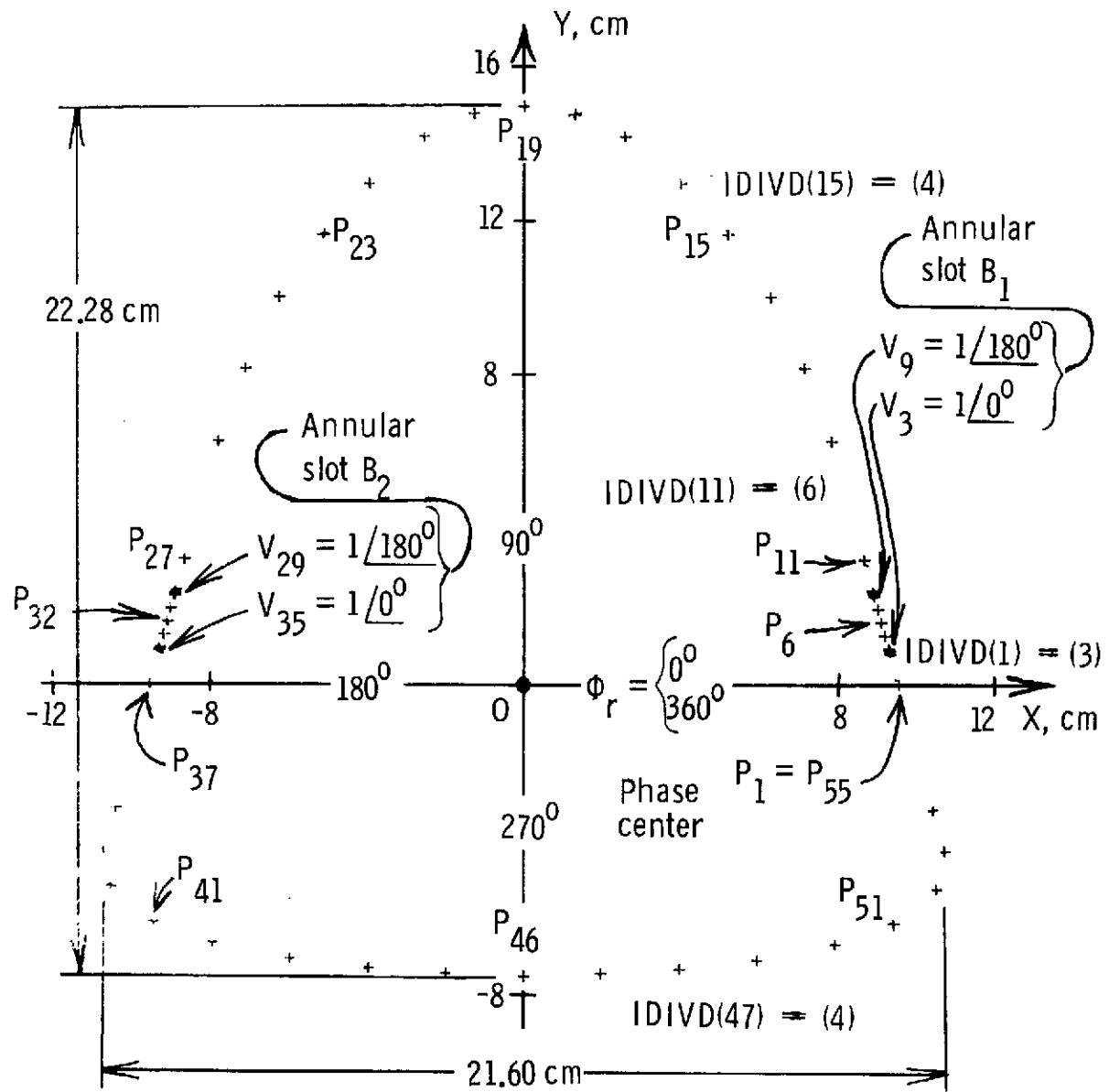


Figure 13.- A plot of the coarse points for case 3; that is, for the example given in appendix B. The coarse points are indexed sequentially as one moves counterclockwise from the positive X-axis. The IDIVD array values are given for selected cases.

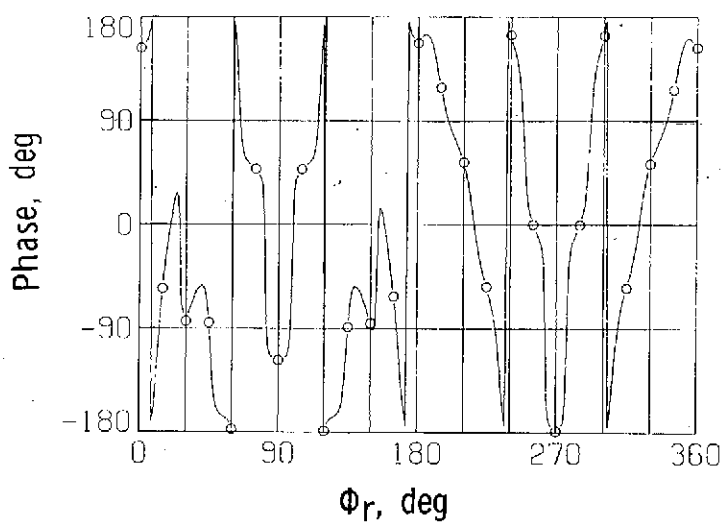
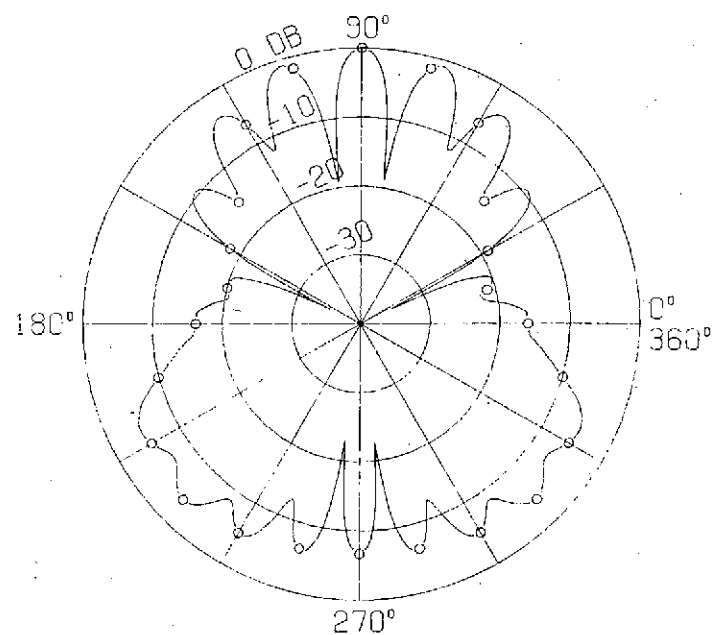


Figure 14.- Graphic output, at a frequency of 5.250 GHz, for the example given in appendix B. The polar plot is a plot of radiation field magnitude in decibels against the roll-plane reference angle in degrees.